NACA RM L54G21

NACA

RESEARCH MEMORANDUM

EFFECTS OF DIFFUSER AND CENTER-BODY LENGTH ON PERFORMANCE OF ANNULAR DIFFUSERS WITH CONSTANT-DIAMETER OUTER WALLS AND WITH VORTEX-GENERATOR FLOW CONTROLS

By Charles C. Wood and James T. Higginbotham

Langley Aeronautical Laboratory
Langley Field, Va.

NATIONAL ADVISORY COMMITTEE FOR AERONAUTICS

WASHINGTON
September 14, 1954

NACA RM L54G21

NATIONAL ADVISORY COMMITTEE FOR AERONAUTICS

RESEARCH MEMORANDUM

EFFECTS OF DIFFUSER AND CENTER-BODY LENGTH ON PERFORMANCE OF ANNULAR DIFFUSERS WITH CONSTANT-DIAMETER OUTER WALLS AND WITH VORTEX-GENERATOR FLOW CONTROLS

By Charles C. Wood and James T. Higginbotham

SUMMARY

Data obtained in a program to determine the performance improvements attainable through the use of boundary-layer controls in annular diffusers applicable to turbojet afterburners are summarized for five diffusers tested with and without vortex-generator controls. The effects on performance of both the diffuser length and the center-body length are emphasized. The diffusers varied in length from an abrupt dump to a length corresponding to an equivalent cone angle of 15°. All diffusers had a constant outer-body diameter of 21 inches, a ratio of outer-body diameter to center-body diameter at the inlet of 1.45, and an area ratio of 1.9 to 1.0. Inlet flow conditions corresponded to a maximum thickness of fully developed turbulent boundary layer, inlet Mach numbers up to 0.4, and both axial flow and 20.6° of whirling flow.

With axial or whirling inlet flow, reductions in diffuser length produced appreciable losses in performance, with or without vortex generators. Vortex generators improved the performance of all diffusers except the abrupt dumps. A diffuser with an outer-body length equivalent to that of the 15° diffuser and a center body about half that length produced slightly less static-pressure rise and somewhat better velocity distributions than the 15° diffuser, with or without vortex generators. With whirling inlet flow, it was necessary to use straighteners to remove most of the whirl in order to avoid large performance penalties.

INTRODUCTION

In a program to determine the performance improvements attainable through use of boundary-layer controls in annular diffusers applicable to turbojet afterburners, five diffusers of different lengths have been tested with and without vortex-generator controls. All diffusers had a constant outer-body diameter of 21 inches, a ratio of outer-body diameter

to center-body diameter at the diffuser inlet of 1.45, and an area ratio of 1.9 to 1.0. The longest diffuser had a conical center body which produced an equivalent cone angle of 15° and was representative of a relatively efficient diffuser. The performance of this diffuser with axial inlet flow is given in reference 1 and with a 21° whirling inlet flow in reference 2. The opposite extreme with respect to length and performance was represented by an abrupt dump, the performance of which is given in reference 3. In order to obtain performance data on two diffuser lengths intermediate between these two extremes, two diffusers with equivalent cone angles of 24° (ref. 4) and 31° were tested. The center body of the 24° diffuser was shaped so as to produce the area variation recommended by Gibson (refs. 5 and 6) for optimum performance. The shape of the center body of the 31° diffuser was arbitrary, and the performance data have not been published previously. The performance with axial inlet flow of a fifth center-body configuration, which was essentially an abrupt dump with the edges rounded to avoid a "vena contracta" effect, is given in reference 7.

The purpose of this paper is to present a concise summary of the performance data for the aforementioned five diffusers in a form which indicates clearly the effects on performance of reducing diffuser length for both axial and whirling inlet flow and with and without vortex generators for flow control. Although the center bodies varied both in length and shape, the comparison of results showing the effect of diffuser length is believed to be valid for engineering purposes.

The diffusers, with the exception of the one of reference 7, were tested under the same inlet conditions: a fully developed turbulent boundary layer extending across the entire inlet annulus; mean inlet Mach numbers up to about 0.4 and corresponding Reynolds numbers based on inlet hydraulic diameter up to 1.28×10^6; and both axial flow and 20.6° of whirling flow. The diffuser of reference 7 was tested under the same conditions for axial flow only.

SYMBOLS

d	diameter of duct
m	mass flow
p	static pressure

$\bar{p}$ weighted static pressure, $\dfrac{\int_{r_1}^{r_2} \rho u p r \, dr}{\int_{r_1}^{r_2} \rho u r \, dr}$

q_c impact pressure, $H - p$

$\bar{q}_c$ mean impact pressure, $\bar{H} - \bar{p}$

r radius of duct

u local velocity measured in direction of flow

$\bar{u}$ mean velocity, $\dfrac{\int_{r_1}^{r_2} u r \, dr}{\int_{r_1}^{r_2} r \, dr}$

y perpendicular distance from either inner or outer walls of diffuser

A cross-sectional area of duct

H total pressure

$\bar{H}$ weighted total pressure, $\dfrac{\int_{r_1}^{r_2} \rho u H r \, dr}{\int_{r_1}^{r_2} \rho u r \, dr}$

L distance downstream from cylinder-diffuser junction

M Mach number

U maximum local velocity at a given duct station

$\frac{\Delta p_2}{\bar{q}_{ci}}$ static-pressure coefficient based on outer-wall static pressures, $\frac{p_2 - \bar{p}_i}{\bar{q}_{ci}}$

$\frac{\overline{\Delta p}}{\bar{q}_{ci}}$ static-pressure coefficient based on weighted static pressures, $\frac{\bar{p} - \bar{p}_i}{\bar{q}_{ci}}$

$\frac{\overline{\Delta H}}{\bar{q}_{ci}}$ loss coefficient, $\frac{\bar{H}_i - \bar{H}}{\bar{q}_{ci}}$

δ boundary-layer thickness

δ^* boundary-layer displacement thickness, $\int_0^{\delta} \left(1 - \frac{u}{U}\right) dy$

θ boundary-layer momentum thickness, $\int_0^{\delta} \frac{u}{U}\left(1 - \frac{u}{U}\right) dy$

$\frac{\delta^*}{\theta}$ boundary-layer shape parameter

ρ mass density

χ whirl angle, measured with respect to the diffuser center line

$\bar{\chi}$ weighted whirl angle, $\frac{\int_{r_1}^{r_2} \rho u \chi r \, dr}{\int_{r_1}^{r_2} \rho u r \, dr}$

Subscripts:

a axial component

d diffuser

e	diffuser exit station
i	diffuser inlet station
t	tailpipe
1	diffuser inner wall
2	diffuser outer wall

CONFIGURATIONS

Diffusers

The same general apparatus and instrumentation was used in all the diffuser investigations and has been described in references 1 to 4 and 7. The general diffuser configuration and station locations are given in figure 1, which is a diagram of diffuser 2. The outer-wall diameter is constant throughout the length of each diffuser and tailpipe. The ratio of the outer-wall diameter to the center-body diameter at the diffuser inlet is 1.45. The diffuser inlet stations were arbitrarily fixed at a point 4 inches upstream from the start of the geometric area expansion in order that the inlet measurements would not be affected measurably by changes in the center-body configurations. The vortex-generator mounting station is located 3 inches downstream from the inlet station in most cases. By definition, the diffuser exit stations are located at the end of each center body. The tailpipe station, which is common to all diffusers, is located 1.262 outer-body diameters from the inlet station or 1.072 diameters from the cylinder-diffuser junction.

Performance data are compared herein for five diffusers which cover a range of equivalent conical expansion angles from 15° to 180°; the corresponding ratios of diffuser length to outer-body diameter L_d/d_2 range from 1.072 to 0. Line drawings of the five configurations and curves of the longitudinal variations of flow area are shown in figure 2. Other pertinent information concerning the diffusers is given in the following table:

Diffuser number	Equivalent conical angle, deg	Diffuser length, L_d/d_2	Tailpipe length, L_t/d_2	Center-body shape
1	15	1.072	0	Conical
2	24	.657	.415	Approximately elliptical
3	31	.506	.566	Approximately elliptical
4	125	.071	1.001	Flat plate with rounded edge
5	180	0	1.072	Abrupt dump

The difference between the length of a particular diffuser and the length of diffuser 1 is referred to as the tailpipe of that diffuser; thus, the length of each diffuser plus its tailpipe is equal to the length of any other diffuser plus its tailpipe $\left(L_d/d_2 + L_t/d_2 = 1.072\right)$. The center-body shapes of diffusers 1, 3, 4, and 5 were arbitrarily selected because of their existence or their simplicity of construction. The center-body shape of diffuser 2 conforms to that recommended by Gibson (refs. 5 and 6) and is intended to produce uniform loss of total pressure per unit of length.

The area-variation plot of figure 2 shows that up to a length corresponding to $0.3L_d/d_2$, the differences in areas between diffusers 1, 2, and 3 are minor. Reference 8 shows that the wall contour in the initial section of a conical diffuser may be varied over a wide range with no measurable effect on the performance; therefore, the differences in shape of the initial sections of diffusers 1, 2, and 3 are believed to be unimportant. Furthermore, the boundary-layer theory given in reference 9 shows that for short diffusers of the type discussed herein the boundary-layer growth characteristics in a diffuser of given length tend to become independent of diffuser shape but become principally a function of area ratio. Therefore, it is believed that the differences in center-body shapes shown in figure 2 are of secondary importance and that any variations in performance are due primarily to differences in diffuser or center-body length.

Vortex Generators

Data are compared herein for only the vortex-generator arrangements which produced the best performance or which illustrate certain important phenomena. Arrangements 1 and 2 (see table I) were used with axial flow, and arrangements 3 and 4 with rotational flow. Arrangement 1 was a counterrotating arrangement (adjacent generators set at angles of opposite sense). Arrangement 2 included arrangement 1 in addition to a second row of counterrotating generators located downstream from the first at approximately the observed separation point with no control. In arrangement 3 (see fig. 3), the purpose of the large-span generators attached to the outer wall was to straighten the flow; whereas, the small-span generators attached to the inner shell were intended to control separation. Arrangement 4 was a corotating arrangement in which the generators were set at a small angle opposite in sense to the direction of rotation. Although it is obvious from table I that complete data are not available for all arrangements for all diffusers, the discussion of the data will indicate that the coverage is sufficient to indicate definite trends of interest.

METHODS OF DATA COMPARISON

Diffuser performances are compared in two general groups: data corresponding to axial inlet flow, and data corresponding to a mean angle of whirl at the inlet of 20.6°. In each case, data are available defining the conditions at two downstream stations, at the end of each center body (the diffuser exit station), and at the fixed tailpipe station corresponding to a length-diameter ratio of 1.072 $\left(L_d/d_2 + L_t/d_2 = 1.072 \right)$. Although the performance parameters are presented herein as a function of L_d/d_2 for the purpose of using a nondimensional quantity, the implication is not intended that L_d/d_2 is a universal parameter or that for a given value of L_d/d_2 the performance of a diffuser of a different type - for instance, one with an expanding outer wall - would be the same as that under discussion. Diffusers which differ moderately from the type investigated, however, would be expected to exhibit qualitatively the same performance trends with diffuser length.

Diffuser performance is given, in general, in terms of three parameters: static-pressure-rise coefficient, total-pressure-loss coefficient, and the radial velocity distributions at the downstream stations. In the cases with axial flow, the static-pressure-rise coefficient $\Delta p_2/\bar{q}_{ci}$ is based on outer-wall static-orifice measurements because radial pressure gradients at the measuring stations were negligible. With whirling flow, the coefficient $\overline{\Delta p}/\bar{q}_{ci}$ is based on mass-weighted survey values in order to account for the large radial pressure gradients. The total-pressure-loss coefficient $\overline{\Delta H}/\bar{q}_{ci}$ is a mass-weighted value in all cases. In the

case of axial flow, the radial velocity distributions at the diffuser exit and tailpipe stations are given in terms of the ratio $u/\bar{u}_i$, which is the ratio of the local velocity at a given radial station to the mean velocity at the inlet station. The local velocity value represents an average of readings from four surveys spaced 90° apart. In the cases with rotational flow, the corresponding parameter $(u/\bar{u}_i)_a$ is presented in terms of the ratio of axial components in order to indicate to a first approximation the radial distribution of mass flow. In addition, longitudinal distributions of wall static pressures and radial distributions at the downstream stations of total and static pressures and the velocity u/U are presented. For the whirling-flow cases, mass-weighted values of whirl angle χ and radial distributions of whirl angle are included in order to complete the description of the flow. The effects of inlet Mach number on performance are indicated by using the pressure ratios, $\bar{p}_i/\bar{H}_i$ for axial flow and $\bar{p}_i/\bar{H}_{ia}$ for whirling flow, as an index to inlet Mach number. An indication of the accuracy of downstream survey measurements is given by comparing values of mass flows based on inlet-station and downstream-station surveys.

RESULTS AND DISCUSSION

Inlet Conditions

Radial distributions of total pressure, static pressure, and whirl angle are presented in figure 4 for an inlet pressure ratio of 0.95. The values plotted are arithmetic averages of measurements made at the four circumferential survey positions. Measurements taken at other inlet pressure ratios indicated no significant variations in the inlet flow conditions. The axial-flow measurements indicate a symmetrical total-pressure distribution with the boundary layers from each wall meeting in the center of the annulus and essentially no static-pressure gradient. For the whirling-flow case, the point of maximum total pressure is closer to the outer wall, the usual static-pressure gradient due to centrifugal force is present, and the angle of whirl is somewhat higher at the outer wall.

The data of figure 4 were converted to velocity distributions and are presented in figure 5 for each of the circumferential survey positions. The values of boundary-layer displacement thickness δ^*, momentum thickness θ, and shape factor δ^*/θ are also presented for axial flow. The conventional interpretations of boundary-layer parameters do not apply for whirling flow; therefore, no values have been presented for this case. The axial-flow parameters indicate some asymmetries relative to δ^* and θ, but the shape factor δ^*/θ varies only ±5 percent and corresponds to low values or distributions most favorable for subsequent diffusion.

Axial Inlet Flow

Flow observation.- The flow along the outer wall of the five diffusers investigated was revealed by tufts to be attached, but the flow along the center bodies of the 15°, 24°, and 31° diffusers appeared to separate at 5, 8, and 4 inches, respectively, downstream from the juncture of the cylinder and center body. Velocity-distribution measurements at the exit of diffuser 1, however, indicated attached flow. Although reattachment of the flow between the 5-inch station and the exit is possible, neither tuft observations nor pressure measurements are regarded as completely reliable for measuring separation points. With vortex generators, the flow along the outer wall of the five diffusers remained attached and appeared to be more stable than with no control. The use of vortex generators moved the separation point for the flow over the center bodies of the 15°, 24°, and 31° diffusers several inches downstream. The two abrupt-expansion diffuser configurations presumably were subject to separated flow in the vicinity of the center-body terminal.

Inlet Mach number effect.- The variation of static-pressure-rise and total-pressure-loss coefficients with inlet pressure ratio is shown by figure 6 to be small and unsystematic for the no-control case. Since inlet Mach number is a unique function of inlet pressure ratio, the variations shown in figure 6 can be identified with inlet Mach number. Within the data accuracy, the range of Mach number tested was not sufficient to draw reliable conclusions regarding Mach number effects. No data are given for diffusers 4 and 5 at the diffuser exit station because, due to the shortness of the center-body configurations, no appreciable diffusion had occurred up to this station. Loss-coefficient data for the tailpipe station of diffuser 4 are also not available. Data taken with vortex generators in place were similar to those of figure 6 and have not been presented. The total-pressure-loss coefficients presented in figure 6 are believed to be too small; this point will be discussed in detail in a subsequent section.

Static-pressure-rise coefficient.- The effect on static-pressure coefficient of reducing diffuser length while maintaining center and outer bodies of equal length is shown by the upper curves of figure 7(a). The static-pressure coefficient decreases rapidly, as the diffuser is shortened, from 0.515 for the 15° diffuser to a negative value for the sharp-edge abrupt-expansion diffuser. The negative coefficient results from a vena contracta effect discussed in references 4 and 7. Vortex-generator arrangements 1 and 2 (see table I) produced significant improvements in the static-pressure coefficient for the three longer diffusers but decreased the coefficients for the two abrupt-expansion diffusers. Arrangement 1, for which data are available for all five diffusers, produced a performance trend with diffuser-length variation similar to the case with no vortex-generator control.

The effect on the static-pressure coefficient of reducing the center-body length while maintaining a fixed outer-body length of 1.072 diameters is shown by the upper curves of figure 7(b). In contrast to the case where the overall length of the diffuser was shortened (fig. 7(a)), the curves of figure 7(b) indicate that shortening the center body to a length-diameter ratio of approximately 0.5 produced only minor decreases in static-pressure coefficient with or without vortex generators. Reducing the center-body length below about 0.5 produced an increasingly rapid rate of depreciation in the coefficient. The values obtained for the abrupt-expansion diffusers for the fixed overall diffuser length (fig. 7(b)) are considerably higher than those of figure 7(a) because of free mixing in the tailpipe downstream from the center-body terminal. Vortex-generator arrangement 1 was responsible for appreciable increases (18 percent for diffuser 1) in the static-pressure coefficient at the tailpipe station; however, the trend as a function of diffuser length was unchanged.

Total-pressure-loss coefficient.- Total-pressure-loss coefficients are presented in figures 7(a) and 7(b) in the lower sets of curves. With the exception of diffuser 1, the loss coefficients measured at the end of the center bodies, figure 7(a), are not considered very realistic because of the poor velocity distributions and high degree of turbulence existing at these stations. The loss coefficients for the case where the overall length of the diffusers was fixed (fig. 7(b)) exhibit, with or without vortex generators, a trend which would normally be expected, increasing loss coefficient with decreased length.

From previous experience in diffuser investigations, it was realized that impact-tube measurements in highly turbulent boundary layers are subject to inherent errors. The nature and magnitude of these errors are described in references 10 and 11 for a wide-angle conical diffuser. For the purposes of the present discussion, it is sufficient to note that the effect of turbulent velocity fluctuations on impact-tube measurements is believed to produce higher total-pressure indications than those associated with the steady through-flow velocity or dynamic pressure. The experimental index to the magnitude of this effect is, therefore, the comparison of the mass-flow measurement at the station in question with a mass-flow measurement of known accuracy, such as the measurement at the diffuser inlet. Figure 8 presents such a comparison for the investigations reported herein.

The apparent mass-flow error (difference between the measured mass flow at the downstream station and the inlet mass flow, expressed as a percentage of the inlet mass flow) is plotted against the length-diameter ratio of the center body for both measuring stations and with and without vortex generators. The values plotted represent averages of those obtained over the Mach number range. The variation with Mach number was a maximum of ±10 percent. Although ordinary experimental inaccuracies, radial flow

components, and flow asymmetries could all contribute to apparent mass-flow discrepancies, the systematic nature of the data indicates that the principal cause was the one previously described.

Although the data of figure 8 cannot be interpreted strictly in terms of turbulence phenomena because the measurements were taken with instrumentation applicable to steady-state conditions only, the implications of the data are of interest. The largest discrepancies were obtained with no control, indicating large turbulence effects due to extensive regions of separated flow. When control was applied, thus reducing the extent of the separated flow, the magnitude of the discrepancies was reduced.

In analyzing the loss-coefficient data, it is necessary to consider the data of figure 8 in conjunction with either figure 6 or 7. Consideration of figures 7 and 8 leads to the following conclusions: the true loss coefficients are probably substantially higher than those shown in figure 7(b); the increase in loss coefficient with shortening of the center body is more rapid than that shown in figure 7; and the use of vortex generators reduced the true loss coefficient for all center-body lengths tested.

No accurate method for correcting the loss-coefficient data exists because turbulence distributions have not been determined and the phenomenon in general has not been evaluated experimentally. If it is imperative that a corrected value of loss coefficient be estimated for purposes of engineering approximations, the use of the following equation is suggested:

$$\left(\frac{\overline{\Delta H}}{\bar{q}_{ci}}\right)_{corrected} = \left(\frac{\overline{\Delta H}}{\bar{q}_{ci}}\right)_{measured} + \frac{(\bar{q}_{ct})_{measured}}{\bar{q}_{ci}}\left[1 - \left(\frac{m_i}{m_t}\right)^2\right]$$

The preceding equation assumes that the measured dynamic pressure at the tailpipe station should be reduced by the square of the ratio of inlet mass flow to measured tailpipe mass flow. Although the accuracy of the proposed correction method is unknown, it is believed that loss coefficients corrected by the method will be more accurate than measured values.

Radial pressure and velocity distributions.- Data on the total-pressure, static-pressure, and velocity distributions are presented in figure 9. Since the static pressure is essentially constant, the principal gradient is in total pressure; thus comparisons can be made in terms of velocity distributions. The velocity distributions are presented

to a larger scale in terms of the mean inlet velocity in figure 10. For reasons previously discussed, the actual velocity ratios were somewhat less than shown in these figures; however, the conclusions to be obtained from these curves are not invalidated.

Velocity distributions measured at the exit stations of the 15°, 24°, and 31° diffusers (diffusers 1, 2, and 3, respectively) and presented in figure 10(a) indicate a steady depreciation as the diffuser length is progressively shortened. For no control, only the data for the 15° diffuser indicate no reverse-flow region; however, this diffuser does have relatively low velocities in a large region near the diffuser center. Control improved the distributions appreciably; the 24° and 31° diffusers still had reverse-flow regions and the 15° diffuser continued to have low velocities in the center, but in smaller regions than for no control.

Velocity distributions at the fixed tailpipe station, shown in figure 10(b), indicate the trend with change in center-body length to be opposite from that noted for change in diffuser length. At the tailpipe station, reductions in center-body length for diffusers 1 to 3 produced improvements in the velocity distributions. At this station, only diffuser 5 had reverse flow (no results are available for diffuser 4). Control improved the distribution for all diffusers and established even greater differences between the profiles for diffusers 3 and 1, with diffuser 3 having a substantially better profile that is probably satisfactory for most applications. With control, the data at the tailpipe station indicate no reverse flow. With regard to the data accuracy, figure 8 shows that the tailpipe-station data with control are most accurate. It may be concluded that the best velocity distribution were produced by a diffuser and tailpipe length of about 1 diameter with a center-body length (L_d/d_2) of about 1/2.

Longitudinal static-pressure distributions.- In order that an indication of the change in flow pattern with length may be obtained, the static pressures along the inner and outer walls of each diffuser tested are presented in figure 11. The data points at the tailpipe station which are connected with the inner-wall pressures were obtained from survey probes located 9.5 inches from the outer wall of the diffuser. Data for the diffusers without vortex generators and with vortex-generator arrangement 1 are presented. For diffusers of the type investigated; all the area expansions take place because of changes to the inner-wall contour; therefore, the inner wall shows the most extreme pressure gradients and the outer-wall pressures result from flow expansion in the region of the inner wall. A local acceleration of flow and a consequent pressure drop occurs because of the rapid change of contour in the vicinity of the juncture between cylinder and diffuser. The boundary layer in the inlet of the diffuser had a relatively good shape and therefore could be subjected to appreciable runs of adverse pressure gradient without separating.

This factor, combined with the initial rapid change in area of the model, resulted in a rapid rate of increase in pressure immediately downstream from the small region possessing accelerated flow. The region of rapid rate of pressure increase extended only a limited distance, however, because the boundary-layer shape became distorted and unable to cope with the adverse pressure gradient. Consequently, flow separation from the inner wall occurred. Downstream from the separation point, the static pressure became constant or, in some cases, decreased slightly, as in the case of diffusers 2 and 3 on the inner wall.

The outer-wall static-pressure measurements were taken over a sufficient length upstream and downstream from the fixed tailpipe station to permit making some observations regarding the optimum lengths of center body and tailpipe. With no control, an overall diffuser length (including the tailpipe) of about 1.2 diameters with a center-body length of about 0.65 diameters is required to recover most of the possible static-pressure rise. With vortex generators, an overall diffuser length of about 1.0 diameter with a center-body length between 0.50 and 0.65 diameters is required to recover most of the possible static-pressure rise.

Once separation occurs, it is improbable that the presence of the inner wall downstream from the line of separation aids the diffusion process. It is quite likely that the rate of diffusion will be increased by dumping the flow at this position, thus providing a free-mixing region equal in area to the diffuser exit area. According to this reasoning, at least the downstream 5 inches of the center body for diffuser 2 and the downstream $4\frac{1}{2}$ inches of the center body for diffuser 3 should be cut off if no control is used. If control is used, at least the downstream 4 and $4\frac{1}{2}$ inches of the center body for diffusers 2 and 3, respectively, should be cut off. For such designs, the center-body terminus should be shaped in such a manner that back flow along the diffuser axis cannot deflect from the end of the center body and introduce radial velocity components into the main flow. A cusp shape similar to the ones illustrated in the sketches of figure 12 is suggested by the discussion of reference 12.

Whirling Inlet Flow

Flow observation.- Flow separation from the inner wall was observed to occur near the end of the center bodies of diffusers 2, 3, and 4 when no generators were used, but was not observed for diffuser 1. Flow along the outer wall remained attached for all tests. The flow angle near the walls increased as the flow proceeded through the diffuser, and the angle of whirl near the inner wall was considerably greater than that near the outer wall. Vortex-generator arrangement 3 established approximately

axial flow on both walls; flow was attached in diffuser 1, but separation was observed on the inner wall near the end of the center bodies of diffusers 2 and 3. Vortex-generator arrangement 4 produced, for both diffusers 1 and 2, flow with large whirl angles near the outer wall and flow near the inner wall which whirled in a direction opposite to that for no control.

Inlet Mach number effect.- The effect of inlet pressure ratio, which may be interpreted in terms of inlet Mach number, on the static-pressure-rise and total-pressure-loss coefficients and on the angle of whirl is presented in figure 13 for the case of whirling inlet flow. All the discussion on inlet Mach number effect for the axial-inlet-flow case also applies directly to the whirling-flow case. The conclusion is that within the data accuracy the range of Mach number tested was not sufficient to draw reliable conclusions regarding Mach number effects.

Static-pressure-rise coefficient.- The effect on static-pressure coefficient of reducing the diffuser length while maintaining inner and outer bodies of equal length is shown by the upper curves of figure 14(a). The trend with diffuser shortening differs somewhat from the axial-flow case in that the differences in static-pressure coefficient between diffusers 1 and 2 are small (L_d/d_2 of 1.072 to 0.657); however, as the length was reduced from a value of 0.657 diameters, a continuous and rapid decrease in the coefficient was obtained. Vortex-generator arrangement 3 increased the static-pressure coefficient in all cases tested; however, the benefit obtained decreased substantially as the diffuser length was reduced. The values of whirl angle measured at the diffuser exit stations and presented in figure 14 indicate that vortex-generator arrangement 3 was effective in removing the whirl motion. Removing the whirl would tend to increase the static-pressure rise irrespective of whether the flow distribution was improved.

The effect on static-pressure coefficient of reducing the center-body length while maintaining a fixed outer-body length of 1.072 diameters is shown for whirling flow by the upper curves of figure 14(b) to be similar to that for axial flow. Only small changes in the coefficient were obtained as the center-body length was reduced from 1.072 diameters to about 0.5 diameter. More rapid decreases in the coefficient were obtained with further shortening. The increase in static-pressure rise obtained with control arrangement 3 became smaller as the center-body length was reduced and became nonexistent for a length of 0.5 diameter. Although no data are available for diffuser 3 ($L_d/d_2 = 0.506$) with arrangement 4, the faired curve through the data for diffusers 1, 2, and 5 indicates that arrangement 4 produced improvements in the static-pressure coefficient over a much wider range of center-body lengths than arrangement 3. Arrangement 4 produced approximately 10 percent improvement in the static-pressure coefficient for L_d/d_2 values ranging from 0.5 to 1.0, as compared to values for arrangement 3 of 20 percent at $L_d/d_2 = 1.0$ and no improvement at $L_d/d_2 = 0.5$.

Total-pressure-loss coefficient.- As in the case for axial flow, the loss-coefficient data of figure 14 should be considered in conjunction with the mass-flow discrepancies of figure 15 in order to arrive at valid conclusions. Figure 15 indicates that the mass-flow discrepancies are larger with control than without and in general are equal for diffuser configurations 1 and 2 but increase rapidly with further shortening of the center body to values as large as 19 percent for the abrupt-expansion configuration. The resulting effect on the loss coefficients is to cause errors small in magnitude for diffuser configurations 1 and 2 and large in magnitude for the configurations with shorter center bodies. This trend causes a more rapid increase in the true loss coefficient with diffuser shortening than that indicated by the measured values of figure 14.

The apparent mass-flow errors for no control are indicated by figure 15 to be negative for diffusers 1, 2, and 3 by a maximum of about 3 percent. Since the mass flow is based on the axial component of the flow, which is calculated by using the cosine of the flow angle, this result is believed to be due to small experimental errors in measuring the very large whirl angles for these cases. In comparison with the axial-flow case with no control, whirling flow with no control produced much lower apparent mass-flow errors and therefore lower true loss coefficients. This result is reasonable since with whirling flow, if the axial component of the velocity is reduced to zero, the whirl component tends to prevent flow separation and the formation of extensive turbulent regions.

The use of vortex generators with whirling flow produced both higher apparent mass-flow errors (fig. 15) and higher loss coefficients (fig. 14). This result is in part a consequence of the turbulence added by the vortex generators to a flow which was basically of a low turbulence level. However, an additional effect may have been responsible for the fact that arrangement 3 produced higher apparent mass-flow errors than arrangement 4. This result is believed to be due to the fact that arrangement 3 removed all the whirl from the flow; whereas, arrangement 4 did not. Thus arrangement 3 permitted the formation of extensive separated-flow regions adjacent to the center body because the flow was approximately axial in this region. The favorable effect on diffuser performance of a whirling flow near the center body has been noted previously for the abrupt-expansion diffuser reported in reference 3. This effect also is believed to be responsible for the differences between arrangements 3 and 4 in the behavior of the static-pressure-rise coefficient (fig. 14(b)) with change in center-body length. It is believed that whirl should be removed from the major portion of the flow at the diffuser inlet in order to recover the energy of whirl, but that a certain amount of whirl should be left in the flow in the region adjacent to the center body. The optimum amount and extent of whirl probably increases as the center body becomes shorter.

Radial pressure and velocity distributions.- Data on the total and static pressures, whirl angles, and velocity distributions are presented in figure 16. At both measuring stations the region of high total pressure loss near the center of the diffusers becomes larger as the center body is shortened; this is generally true even when controls are used. The radial static-pressure gradients, which are caused by the whirl-angle distributions, are large for no control and decrease with diffuser shortening. With control, the distribution depends mostly on the control configurations; arrangements 3 and 4 largely eliminate this gradient for all except diffuser 5. Reduction in diffuser length produced unfavorable changes in the velocity distribution at the diffuser exit stations for both control and no control. At the tailpipe station, the change in velocity distribution with center-body shortening was small with no control. With control, the longer center bodies produced more favorable profiles.

The distribution of axial velocity components as a function of the mean upstream axial velocity component is presented in figure 17. Certain diffuser configurations have mean velocities somewhat greater than other configurations because of the mass-flow discrepancies previously discussed; however, general conclusions are not invalidated. The diffuser-exit data of figure 17(a) indicate increasing distortion of the velocity distribution with progressive shortening of the diffuser. With no control, each diffuser had a region of no positive axial flow near the duct center line. Vortex generators eliminated this region for diffuser 1 but did not appreciably improve the distributions for diffusers 2 and 3.

The velocity distributions at the fixed tailpipe station for all center-body lengths except number 5 are approximately the same with no control. Each has a small region of no axial flow near the duct center line. Control improves the velocity distributions and eliminates the regions of no axial flow. The curves indicate that the longer center bodies produce somewhat better distributions. This trend is accentuated by the mass-flow-discrepancy data. The mixing accomplished in the tailpipe section produces appreciable improvements in the velocity distributions.

Longitudinal static-pressure distributions.- Longitudinal variations of static pressure along the inner and outer walls are presented in figure 18 for all configurations with and without control. A comparison of figures 11 (axial flow) and 18 will show that the large radial pressure gradients set up by the whirling motion influenced the longitudinal gradients to a high degree, especially on the inner wall. This effect prohibits correlation of the curves relative to flow separation in a manner similar to the axial-flow correlation.

CONCLUSIONS

The following conclusions are drawn as to the effect of diffuser length and center-body length on the performance of annular straight-outer-wall diffusers with an area ratio of 1.9 to 1 and with and without vortex generators for control. The investigation was conducted with fully developed pipe flow at the inlet for axial inlet flow and for an inlet angle of whirl of 20.6°.

With axial inlet flow:

1. As the diffuser length was reduced (maintaining center bodies and outer bodies of equal length) from a length-diameter ratio of approximately 1.0 (conical expansion angle of 15°) to zero, a progressive and appreciable decrease in static-pressure rise and deterioration in exit velocity distribution was obtained with or without vortex generators.

2. Vortex generators improved significantly the performance of the three longer diffusers, which had conical expansion angles of 15°, 24°, and 31°.

3. Pressure surveys at the exit station indicated that the flow did not separate from the center body of the 15° diffuser, with or without vortex generators. An appreciable portion of the downstream end of the center bodies of the 24° and 31° diffusers was ineffective in the diffusion process because of flow separation.

4. The combination of the 31° diffuser and tailpipe, which is equivalent in length to the 15° diffuser, produced slightly less static-pressure rise and somewhat better velocity distributions than the 15° diffuser, with or without vortex generators. This result indicates that for an overall diffuser length (including tailpipe) of about 1.0 outer diameter, the center-body length should be about one-half the overall length for diffusers of the type investigated.

With whirling inlet flow:

5. As the diffuser length was reduced (maintaining center bodies and outer bodies of equal length) from a length-diameter ratio of 0.66 (conical expansion angle of 24°) the static-pressure-rise coefficient decreased rapidly with or without vortex generators; the exit velocity distribution became progressively less uniform with diffuser shortening with or without vortex generators.

6. Vortex generators improved significantly the static-pressure-rise coefficient of the longer diffusers and the velocity distribution at the fixed tailpipe station for all center bodies tested except the abrupt-expansion case.

7. The combination of the 31° diffuser and tailpipe produced slightly less static-pressure rise than the 15° diffuser for both no control and the vortex-generator arrangement which did not remove all the whirl from the flow.

Langley Aeronautical Laboratory,
National Advisory Committee for Aeronautics,
Langley Field, Va., July 2, 1954.

REFERENCES

1. Wood, Charles C.: Preliminary Investigation of the Effects of Rectangular Vortex Generators on the Performance of a Short 1.9:1 Straight-Wall Annular Diffuser. NACA RM L51G09, 1951.

2. Wood, Charles C., and Higginbotham, James T.: The Influence of Vortex Generators on the Performance of a Short 1.9:1 Straight-Wall Annular Diffuser With a Whirling Inlet Flow. NACA RM L52L01a, 1953.

3. Wood, Charles C., and Higginbotham, James T.: Flow Diffusion in a Constant-Diameter Duct Downstream of an Abruptly Terminated Center Body. NACA RM L53D23, 1953.

4. Wood, Charles C., and Higginbotham, James T.: Performance Characteristics of a 24° Straight-Outer-Wall Annular-Diffuser-Tailpipe Combination Utilizing Rectangular Vortex Generators for Flow Control. NACA RM L53H17a, 1953.

5. Gibson, A. H.: On the Flow of Water Through Pipes and Passages Having Converging or Diverging Boundaries. Proc. Roy. Soc. (London), ser. A, vol. 83, no. 563, March 2, 1910, pp. 366-378.

6. Gibson, A. H.: On the Resistance to Flow of Water Through Pipes or Passages Having Divergent Boundaries. Trans. Roy. Soc., Edinburgh, vol. 48, part I, no. 5, 1911, pp. 97-113.

7. Henry, John R., and Wilbur, Stafford W.: Preliminary Investigation of the Flow in an Annular-Diffuser—Tailpipe Combination With an Abrupt Area Expansion and Suction, Injection, and Vortex-Generator Flow Controls. NACA RM L53K30, 1954.

8. Copp, Martin R.: Effects of Inlet Wall Contour on the Pressure Recovery of a 10° 10-Inch-Inlet-Diameter Conical Diffuser. NACA RM L51E11a, 1951.

9. Rubert, Kennedy F., and Persh, Jerome: A Procedure for Calculating the Development of Turbulent Boundary Layers Under the Influence of Adverse Pressure Gradients. NACA TN 2478, 1951.

10. Persh, Jerome, and Bailey, Bruce M.: Effect of Various Arrangements of Triangular Ledges on the Performance of a 23° Conical Diffuser at Subsonic Mach Numbers. NACA TN 3123, 1954.

11. Persh, Jerome, and Bailey, Bruce M.: A Method for Estimating the Effect of Turbulent Velocity Fluctuations in the Boundary Layer on Diffuser Total-Pressure-Loss Measurements. NACA TN 3124, 1954.

12. Ringleb, F. O.: Theory and Application of the Flow Over a Cusp. Rep. 192, Princeton Univ., Dept. of Aero. Eng., Mar. 1952.

TABLE I

VORTEX-GENERATOR ARRANGEMENTS

[NACA 0012 rectangular, untwisted airfoils]

Arrangement	No. of generators	Chord, in.	Span, in.	Angle setting, deg	Location upstream (+) or downstream (-) from cylinder-diffuser junction, in.	Wall	Diffuser 1	2	3	4	5
1	24	3	$\frac{1}{2}$	±15	+1 or +4 [a]	Inner	x	x	x	x	x
2	24	3	$\frac{1}{2}$	±15	+1	Inner					
	(b)	2	$\frac{1}{2}$	±15	(b)	Inner		x	x		
3	24	3	$3\frac{1}{8}$	0	+2	Outer					
	24	3	$\frac{1}{2}$	±15	+1	Inner	x	x	x		
4	24	3	$1\frac{9}{16}$	-4	+1 or +4 [a]	Inner	x	x			x

[a]Generators for all diffusers except diffuser 5 were located at +1.

[b]Diffuser 2 had 20 vortex generators located at -7 inches; diffuser 3 had 24 vortex generators located at -4 inches.

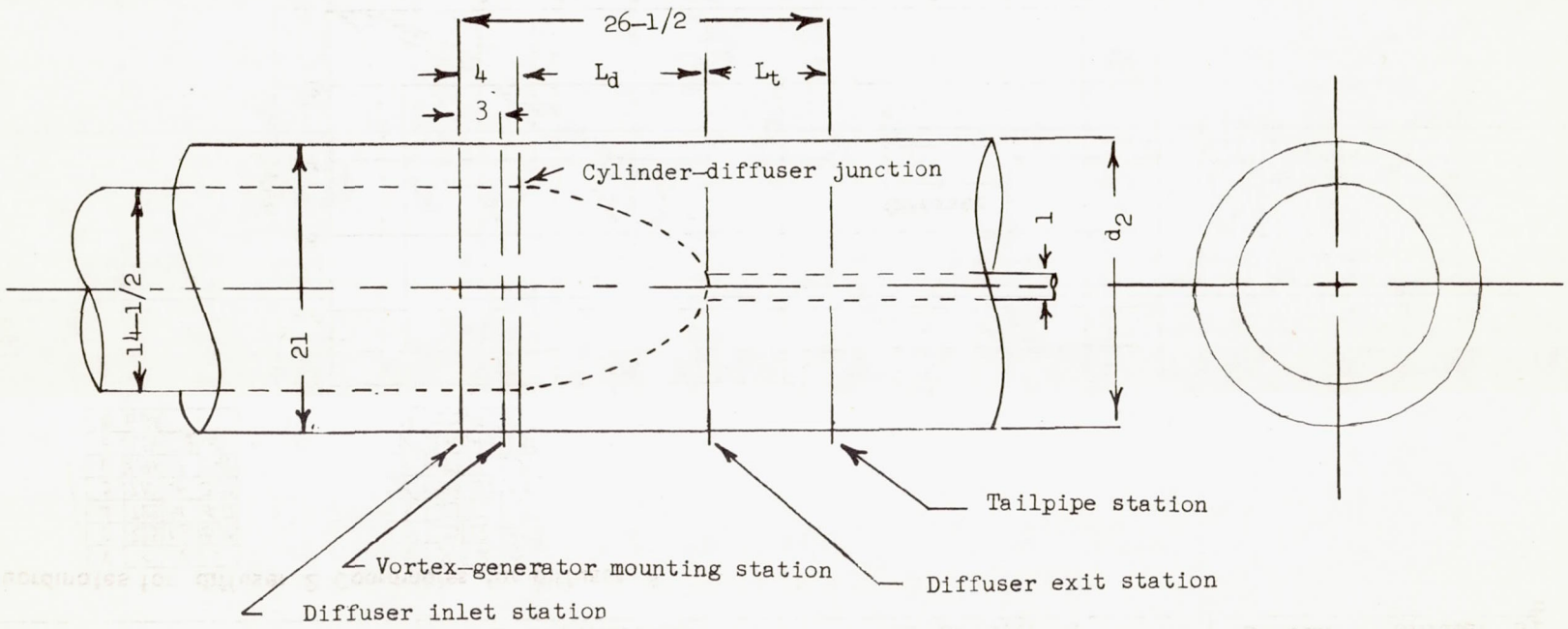

Figure 1.- Schematic diagram of diffuser 2. All dimensions are in inches.

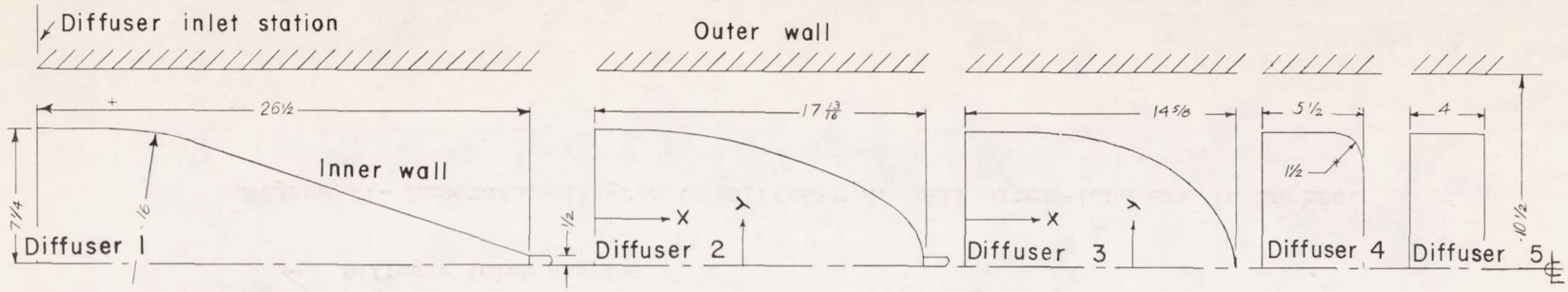

Coordinates for diffuser 2

X	Y	X	Y
0	7.25	12	5.35
4	7.25	14	4.57
5	7.10	16	3.21
6	6.94	17	2.41
8	6.54	17 13/16	0
10	6.04		

Coordinates for diffuser 3

X	Y	X	Y
0	7.25	12	4.47
4	7.25	13	3.57
6	7.08	13½	2.96
8	6.59	14	2.21
10	5.81	14½	0.94
11	5.23	14 5/8	0

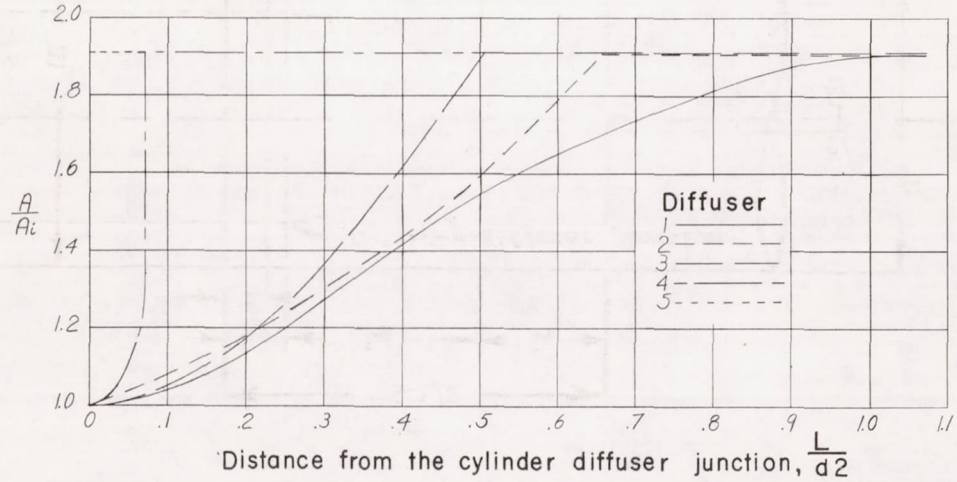

Figure 2.- Schematic view and area-distribution curve of each of the five diffusers investigated. All dimensions are in inches.

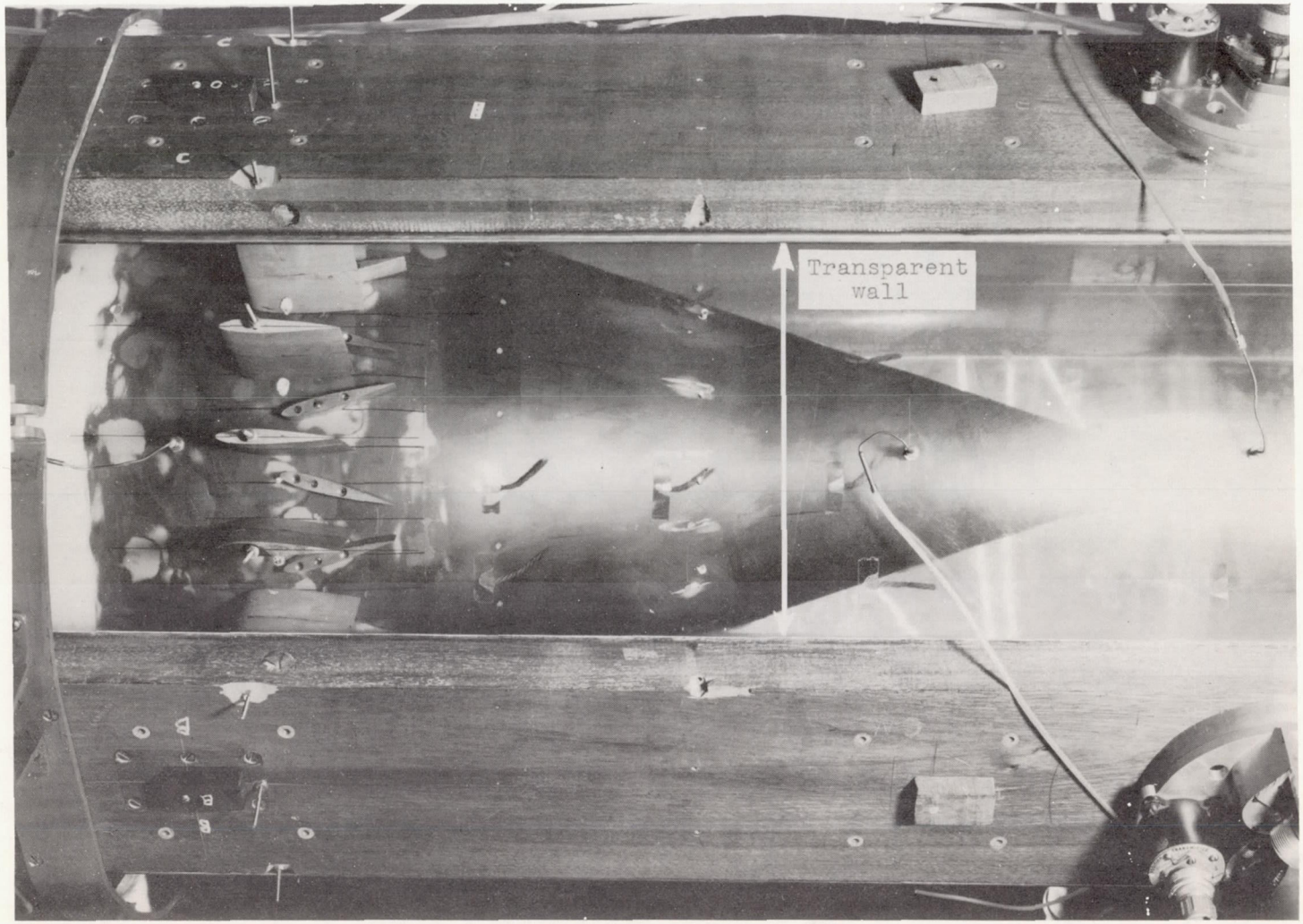

L-74511.1

Figure 3.- Diffuser 1 with vortex generators on both the inner and outer walls (vortex-generator arrangement 3).

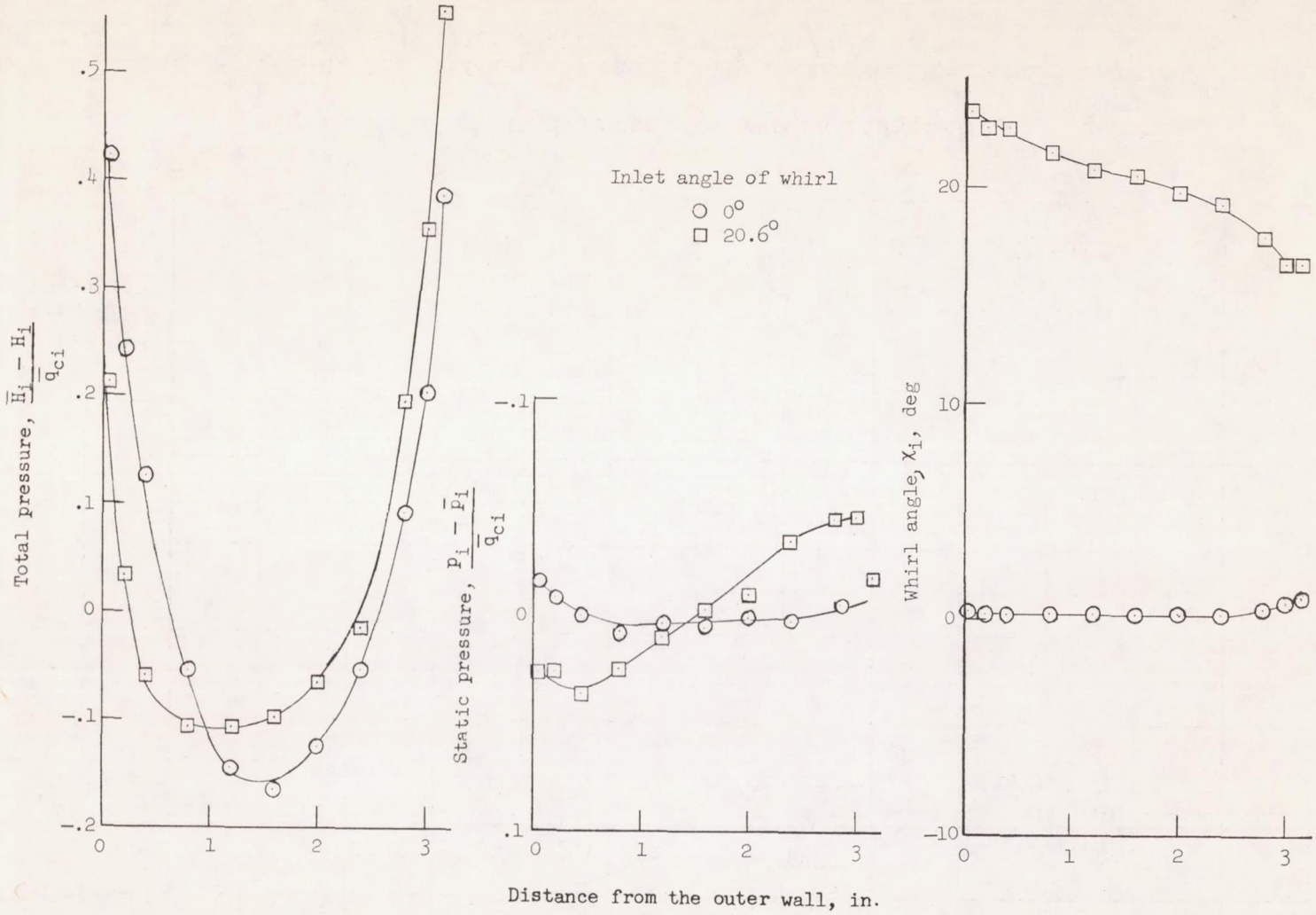

Figure 4.- Radial variations of total pressure, static pressure, and whirl angle at the diffuser inlet for two inlet-whirl angles. $\bar{p}_i/\bar{H}_{ia} = 0.95$.

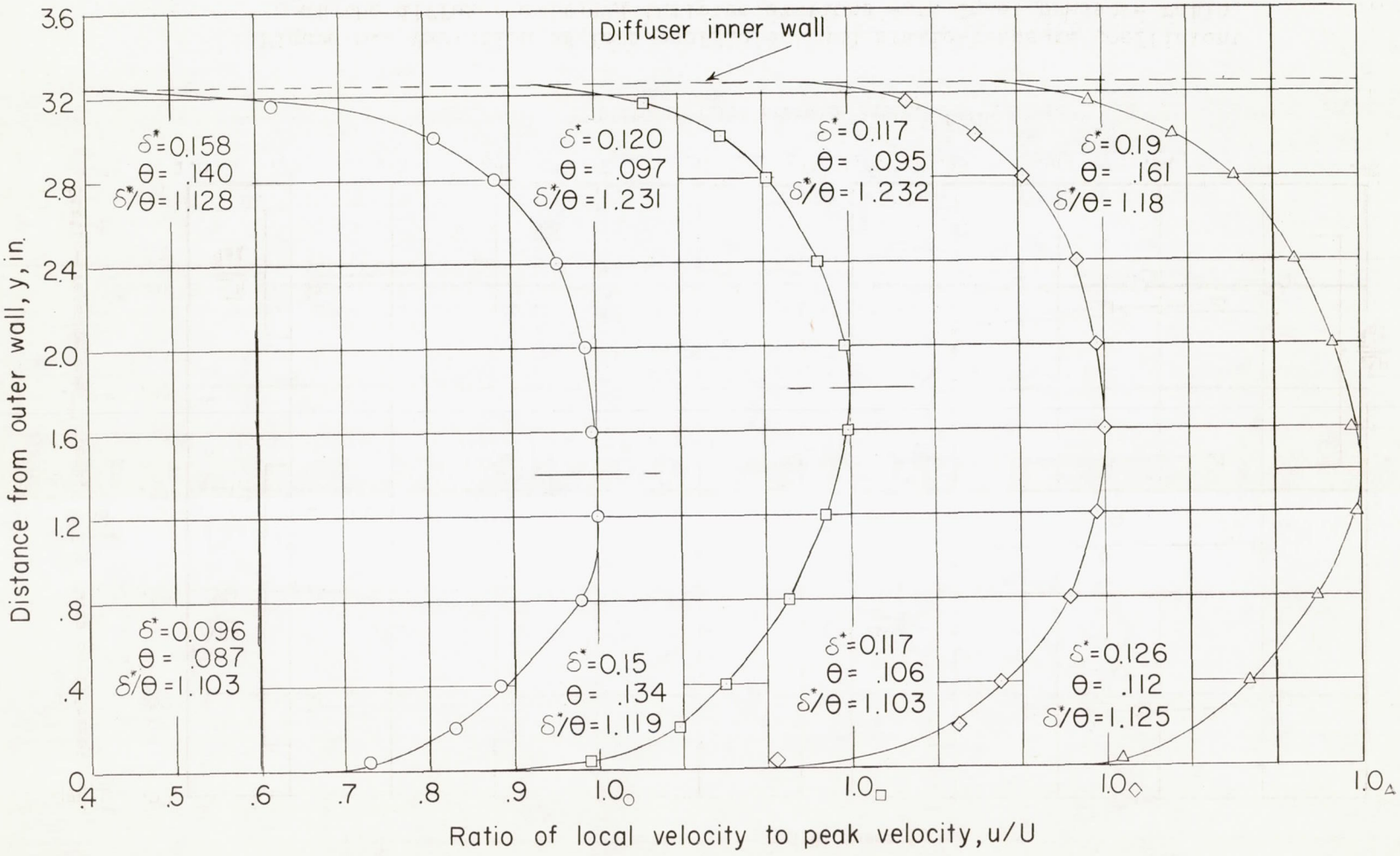

Figure 5.- Velocity profiles at four equally spaced sections around the diffuser inlet station. $\bar{X}_i = 0^o$; $\bar{p}_i/H_i = 0.95$.

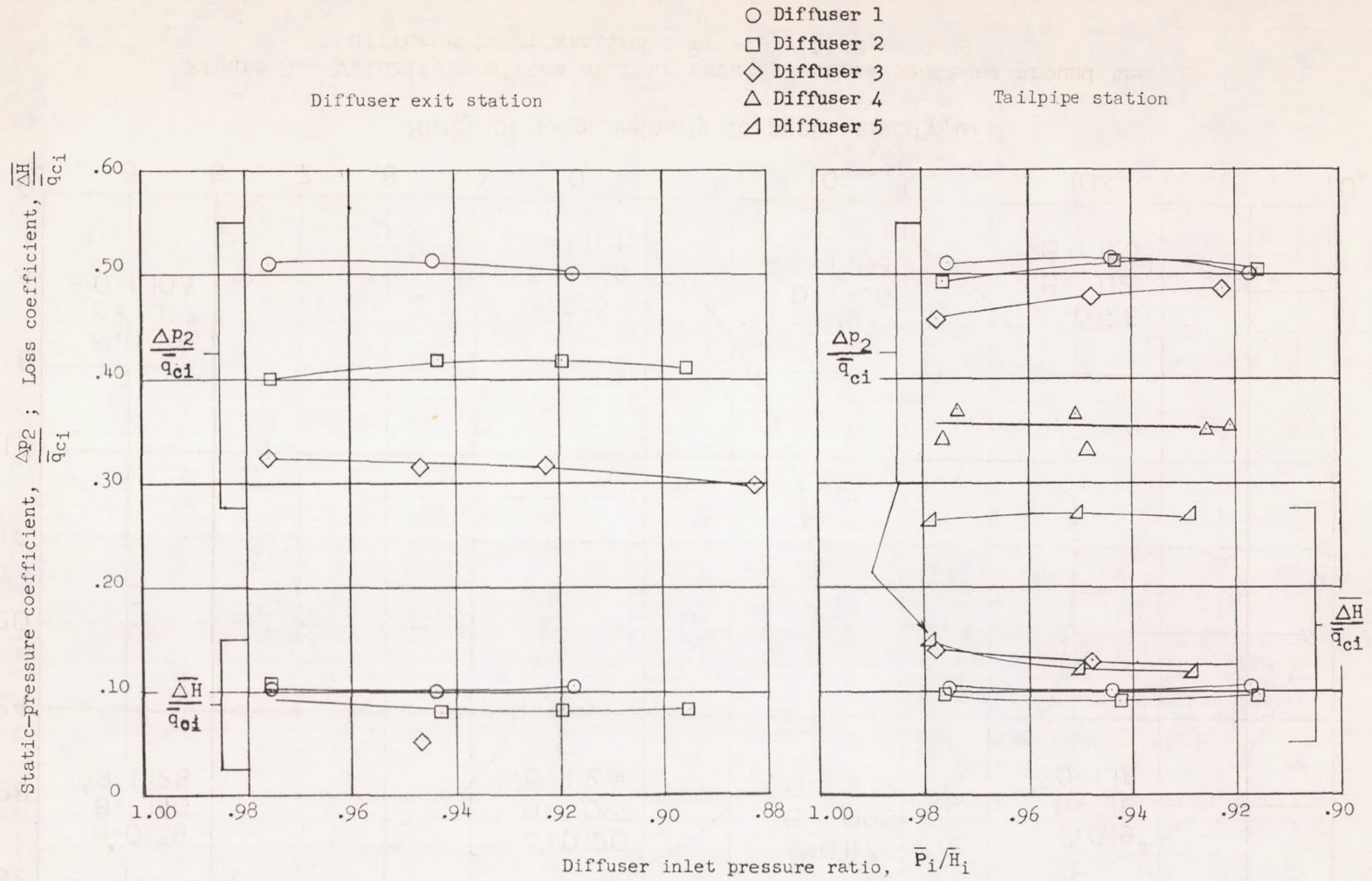

Figure 6.- Variation of loss coefficient and static-pressure coefficient at the diffuser exit and tailpipe stations with inlet pressure ratio for each of the five diffusers without vortex generators. $\bar{\chi}_i = 0^\circ$.

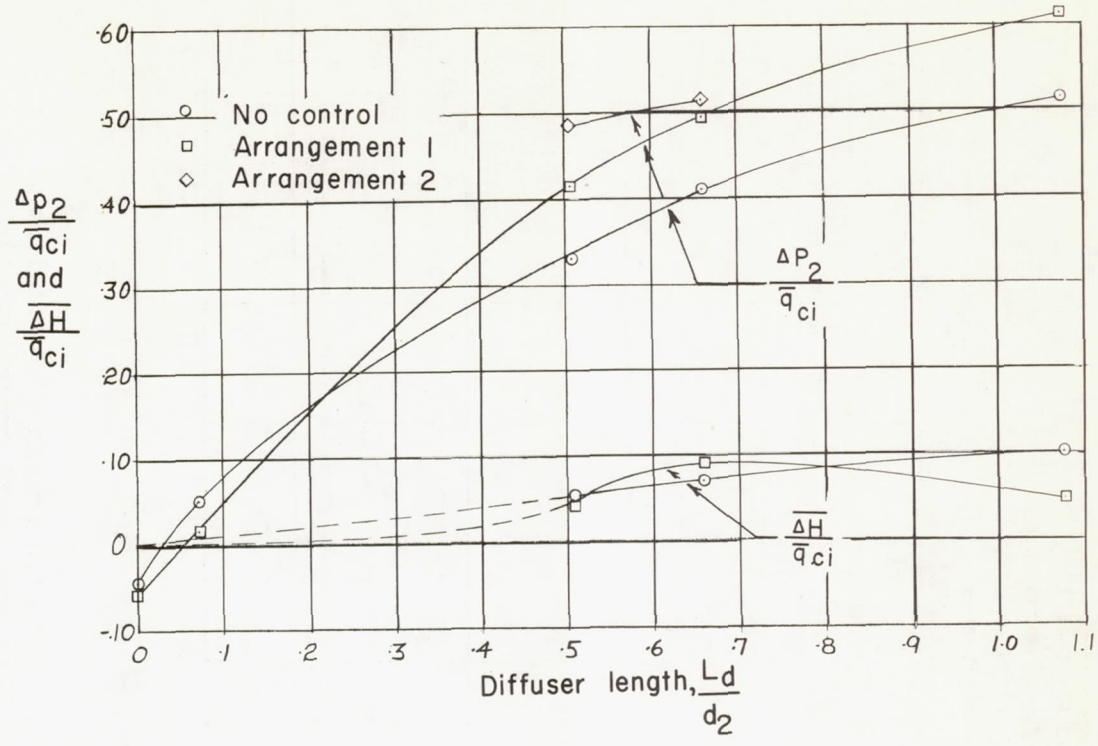

(a) Measurements to diffuser exit station; variable diffuser length.

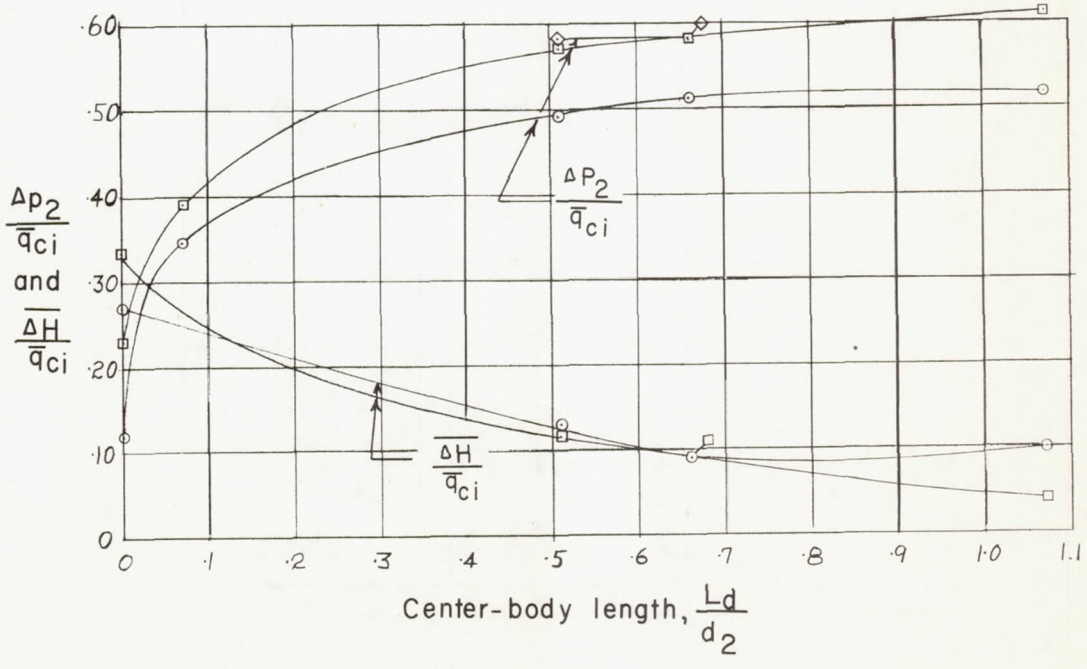

(b) Measurements to fixed tailpipe station; variable center-body length.

Figure 7.- Variations of the static-pressure and loss coefficients with diffuser and center-body length. $\bar{\chi}_i = 0^\circ$; $\bar{p}_i/\bar{H}_i = 0.94$.

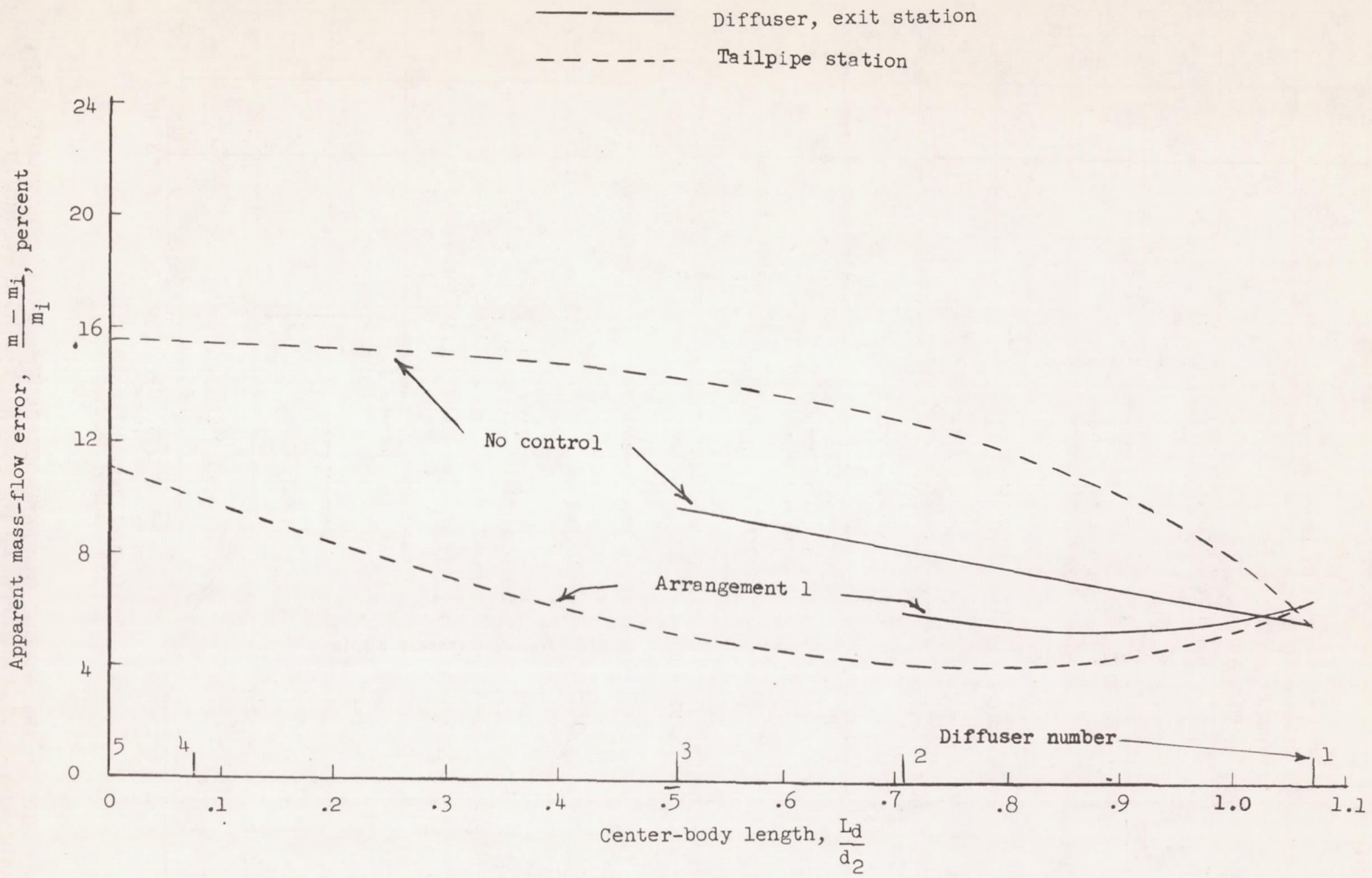

Figure 8.- Effects of center-body length on the apparent errors in mass flow between the inlet station and survey stations located downstream. $\bar{x}_i = 0^\circ$; $\bar{p}_i/\bar{H}_i = 0.95$.

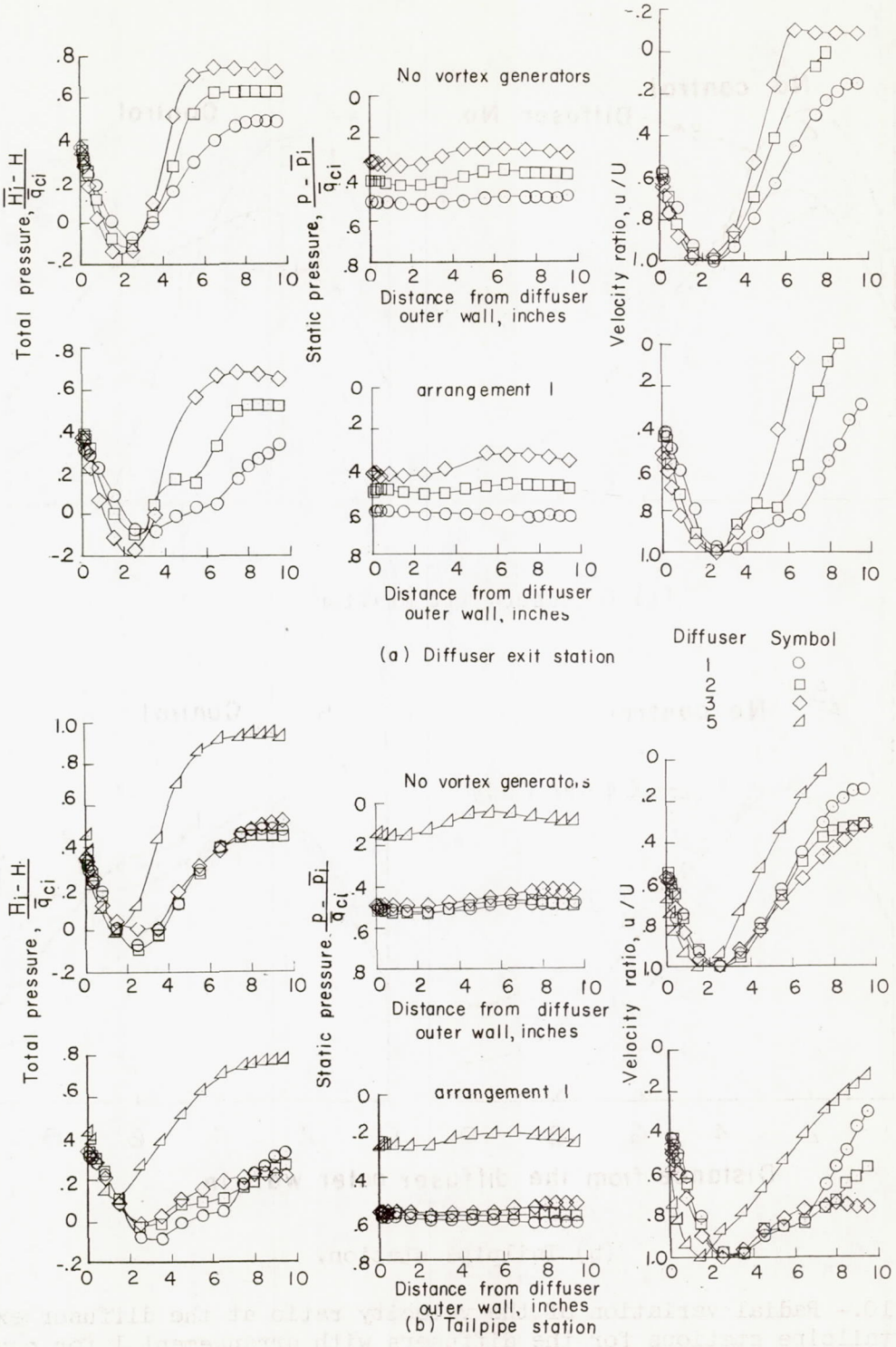

Figure 9.- Radial variations of total pressure, static pressure, and velocity ratio at the diffuser exit and tailpipe stations. $\chi_i = 0^\circ$; $\bar{p}_i/\bar{H}_i = 0.95$.

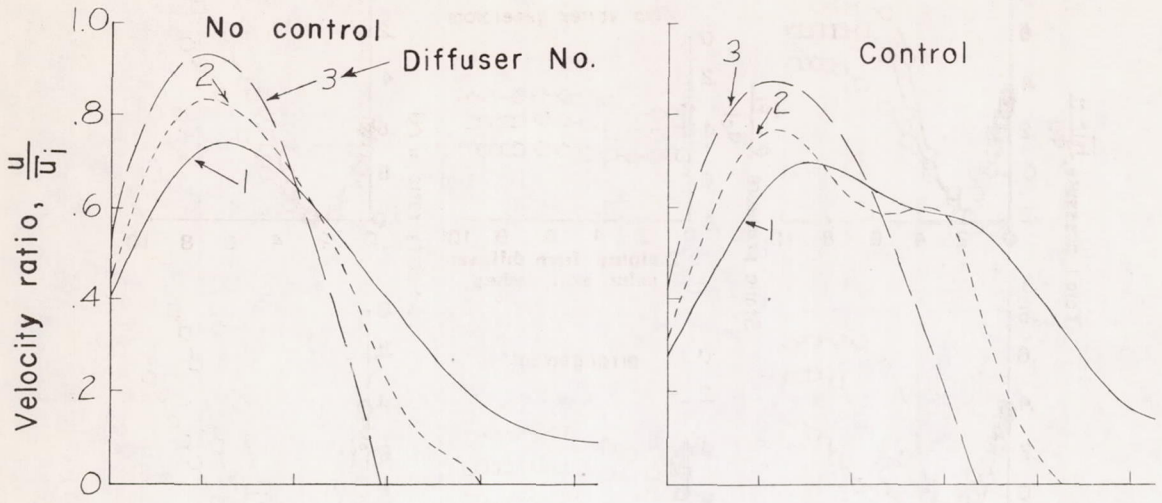

(a) Diffuser-exit station.

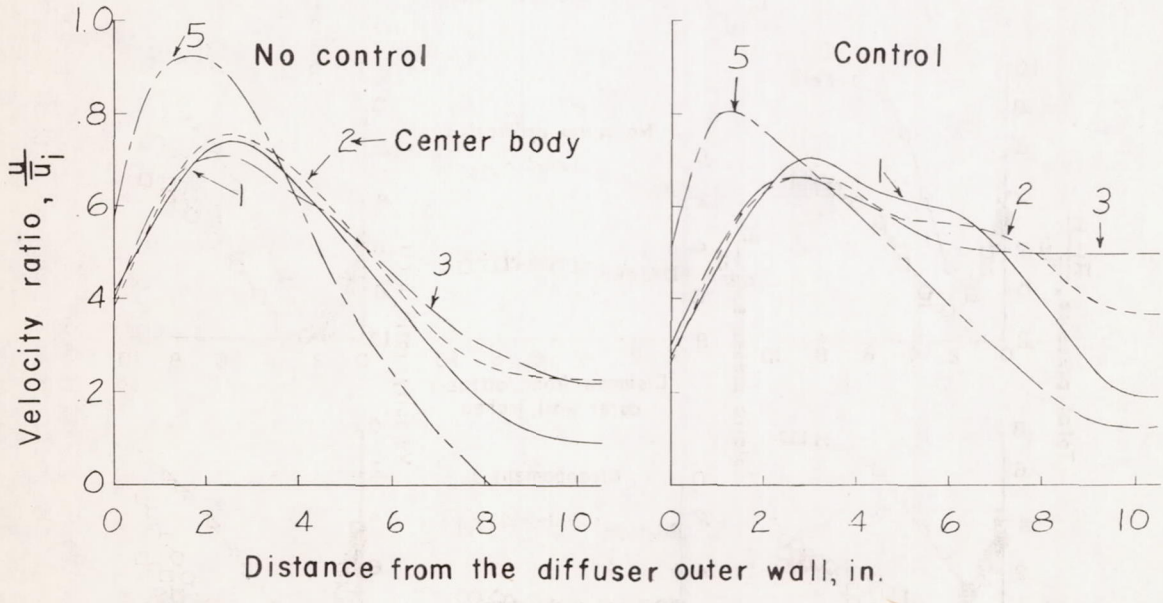

(b) Tailpipe station.

Figure 10.- Radial variation of the velocity ratio at the diffuser exit and tailpipe stations for the diffusers with arrangement 1 for control and without control. $\bar{\chi}_i = 0^\circ$; $\bar{p}_i/\bar{H}_i = 0.95$.

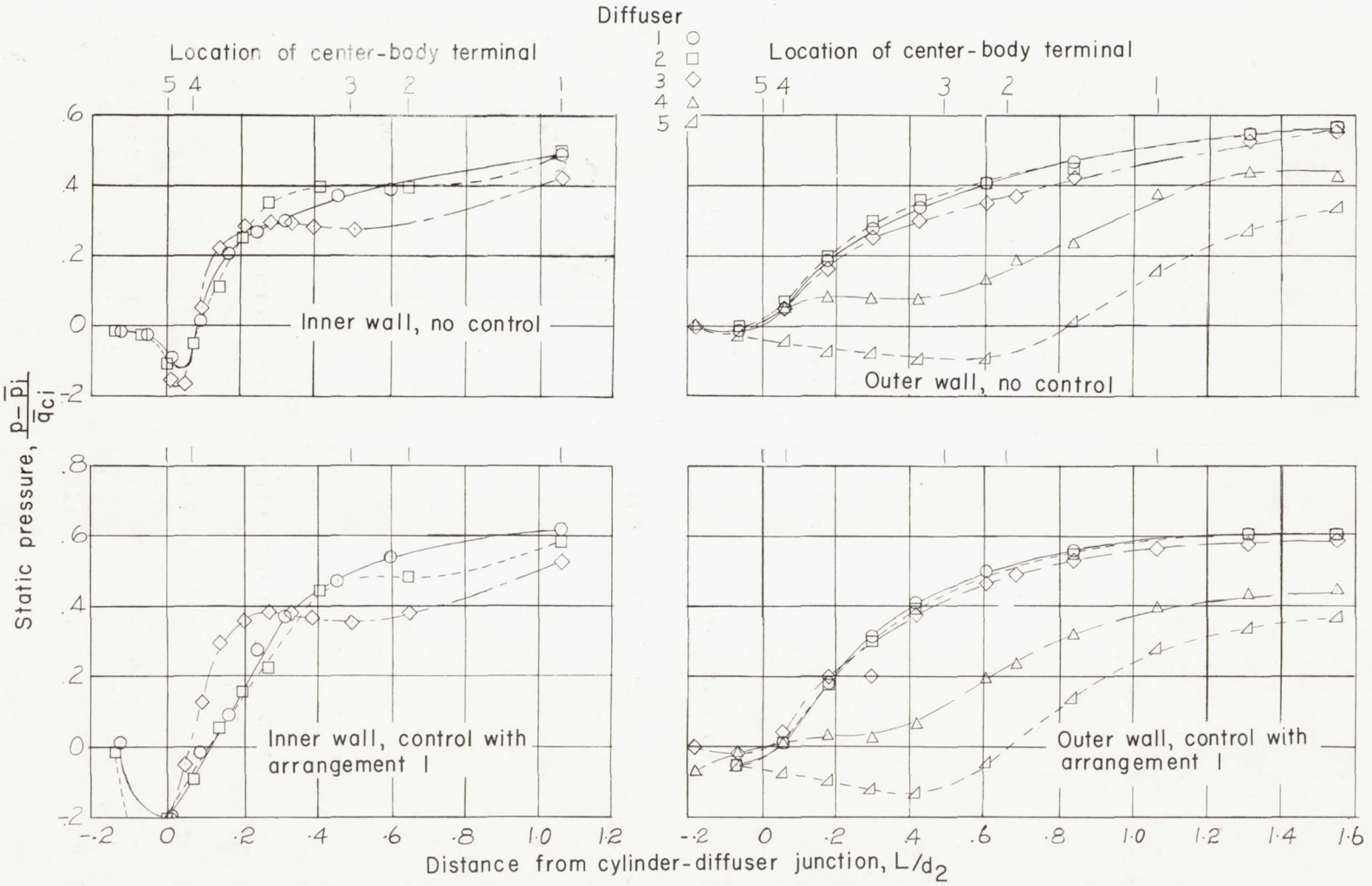

Figure 11.- Variation of static pressure along the inner and outer walls of the diffusers with and without vortex generators. $\bar{X}_i = 0^o$; $\bar{p}_i/H_i = 0.95$.

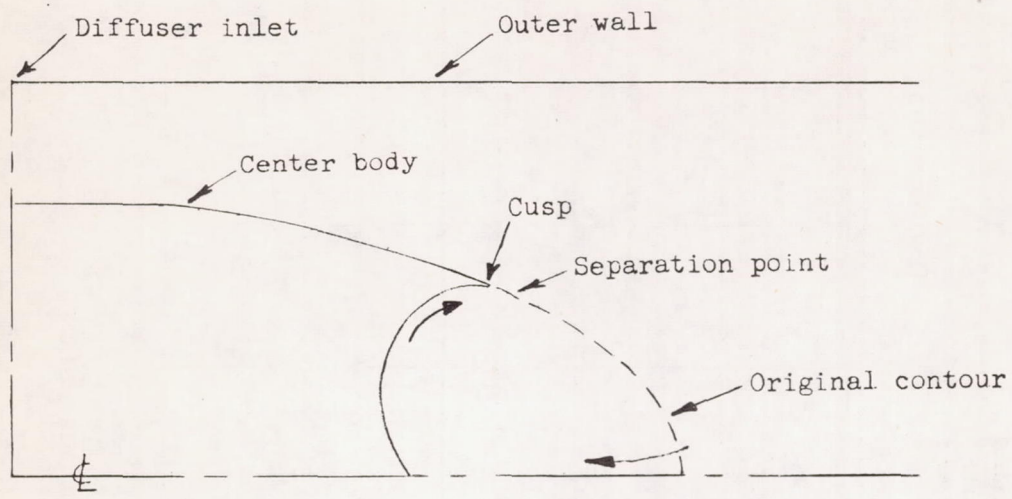

(a) Diffuser 2; equivalent cone angle, 24°.

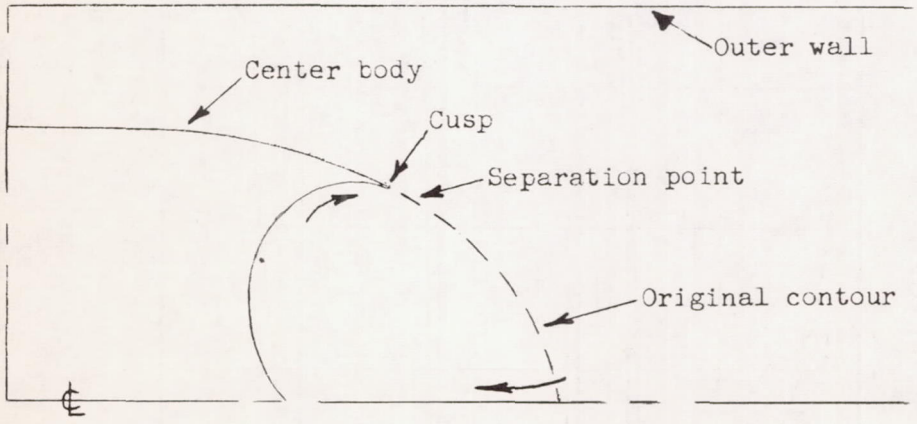

(b) Diffuser 3; equivalent cone angle, 31°.

Figure 12.- Sketches of suggested method for terminating center body at separation point.

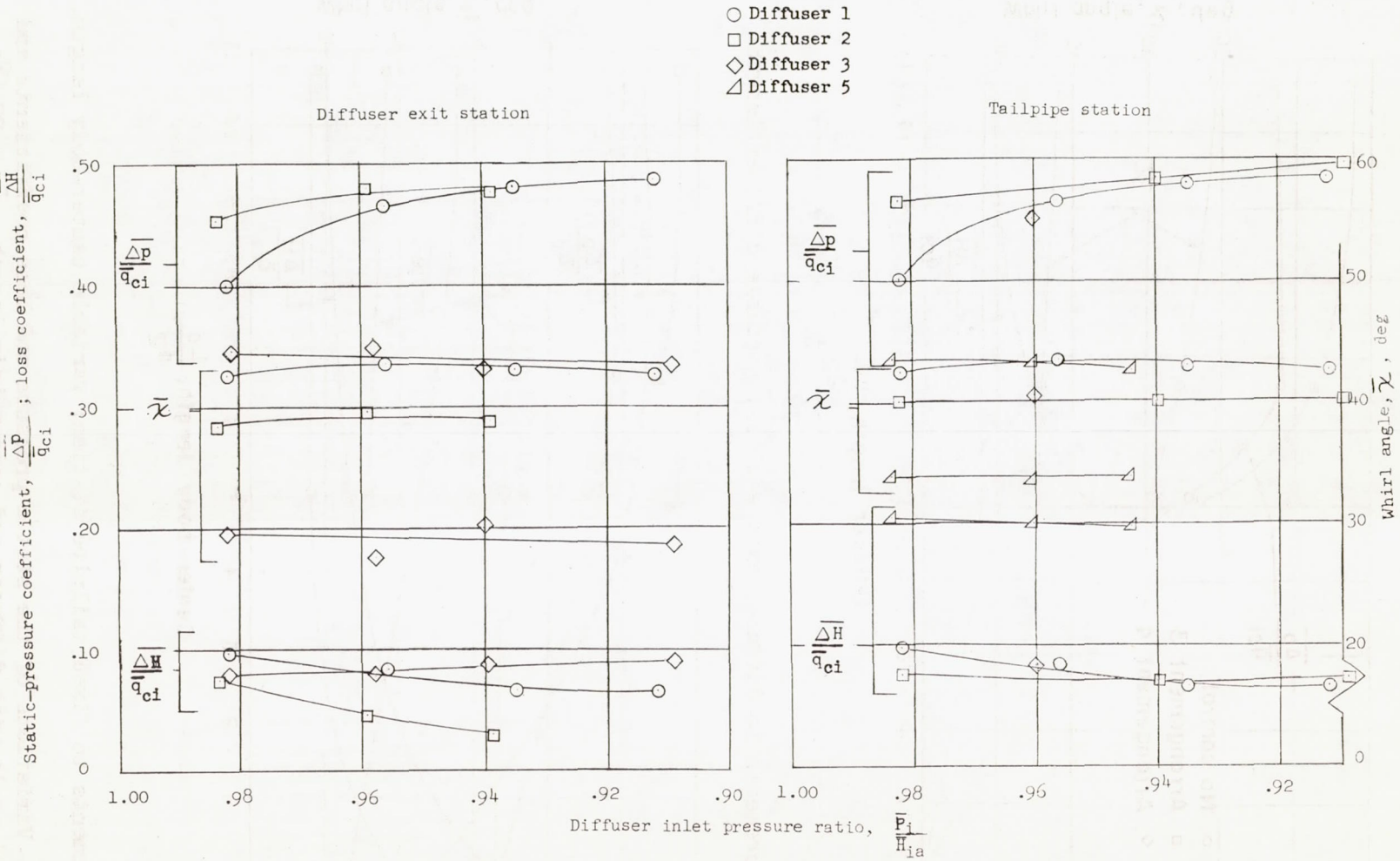

Figure 13.- Variation of loss coefficient, static-pressure coefficient, and whirl angle at the diffuser exit and tailpipe stations with inlet pressure ratio for each of the diffusers without vortex generators. $\bar{X}_i = 20.6^\circ$.

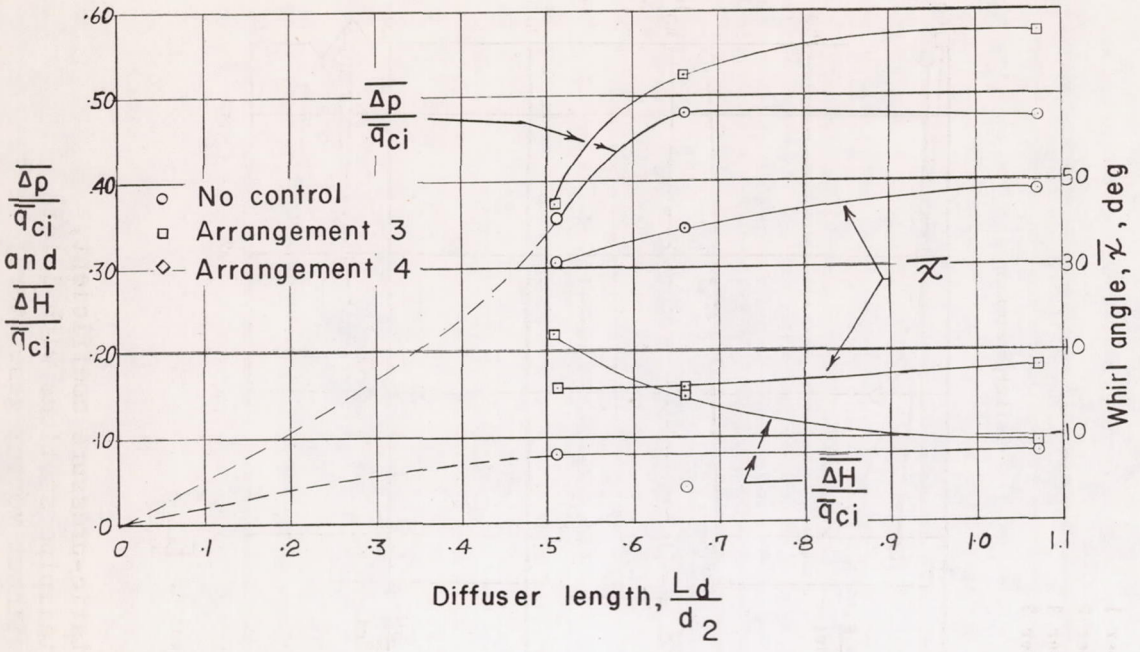

(a) Measurements to diffuser exit station; variable diffuser length.

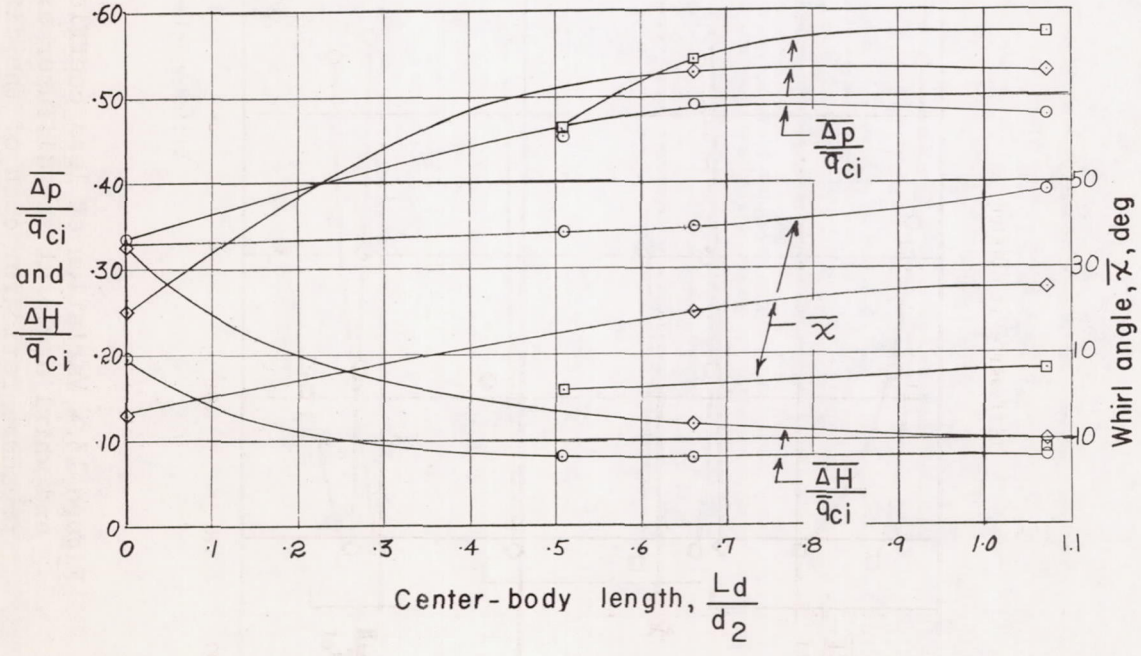

(b) Measurements to fixed tailpipe station; variable center-body length.

Figure 14.- Variations of the static pressure and loss coefficients and the whirl angle with diffuser and center body length. $\bar{\chi}_i = 20.6^\circ$; $\bar{p}_i/H_{ia} = 0.95$.

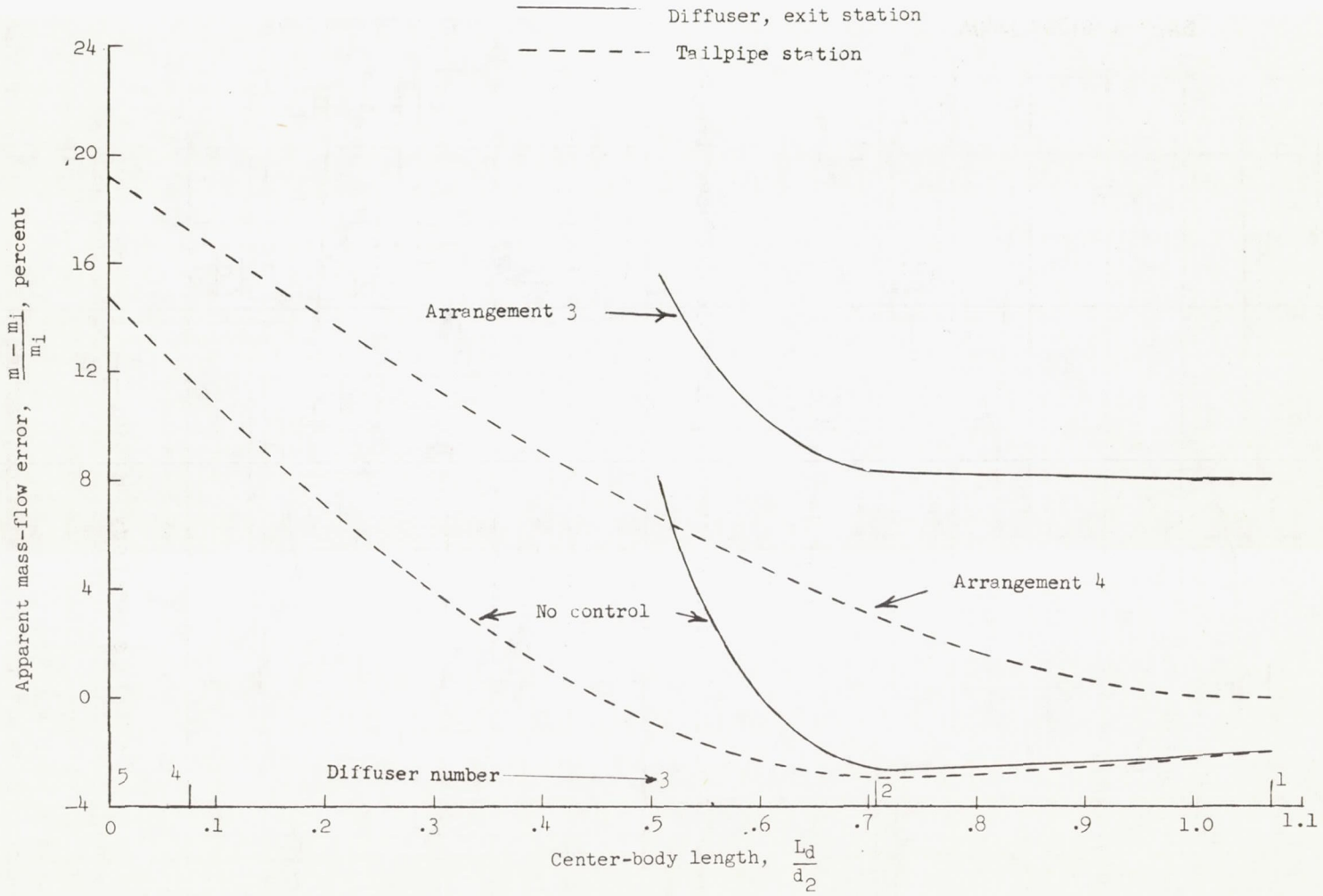

Figure 15.- Effects of center-body length on the apparent errors in mass flow between the inlet station and survey stations located downstream. $\bar{X}_i = 20.6^\circ$; $\bar{p}/\bar{H}_{ia} = 0.95$.

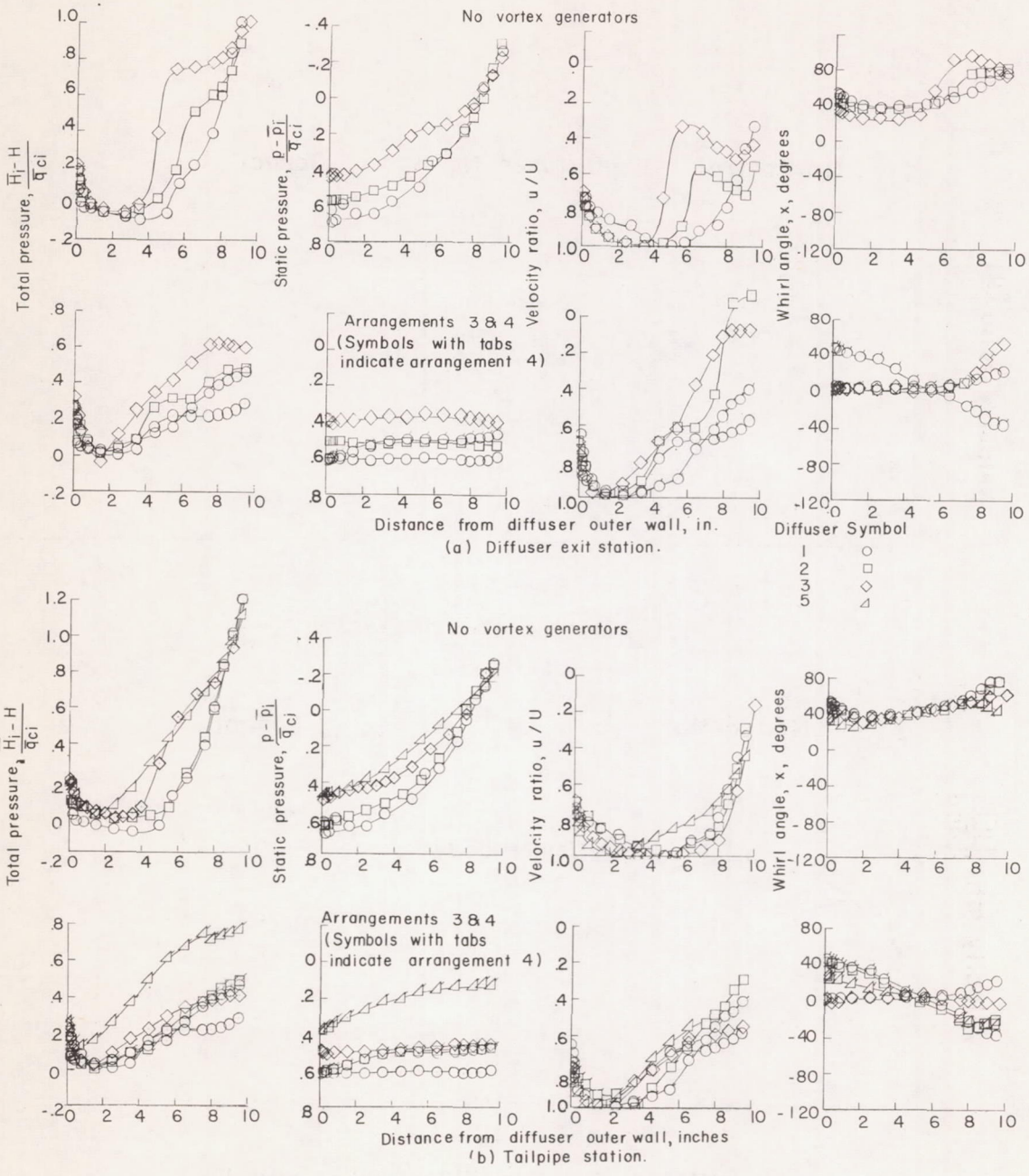

Figure 16.- Radial variation of total pressure, static pressure, velocity ratio, and whirl angle at both the diffuser exit and tailpipe stations. $\bar{\chi}_i = 20.6^\circ$; $\bar{p}_i/\bar{H}_{ia} = 0.96$.

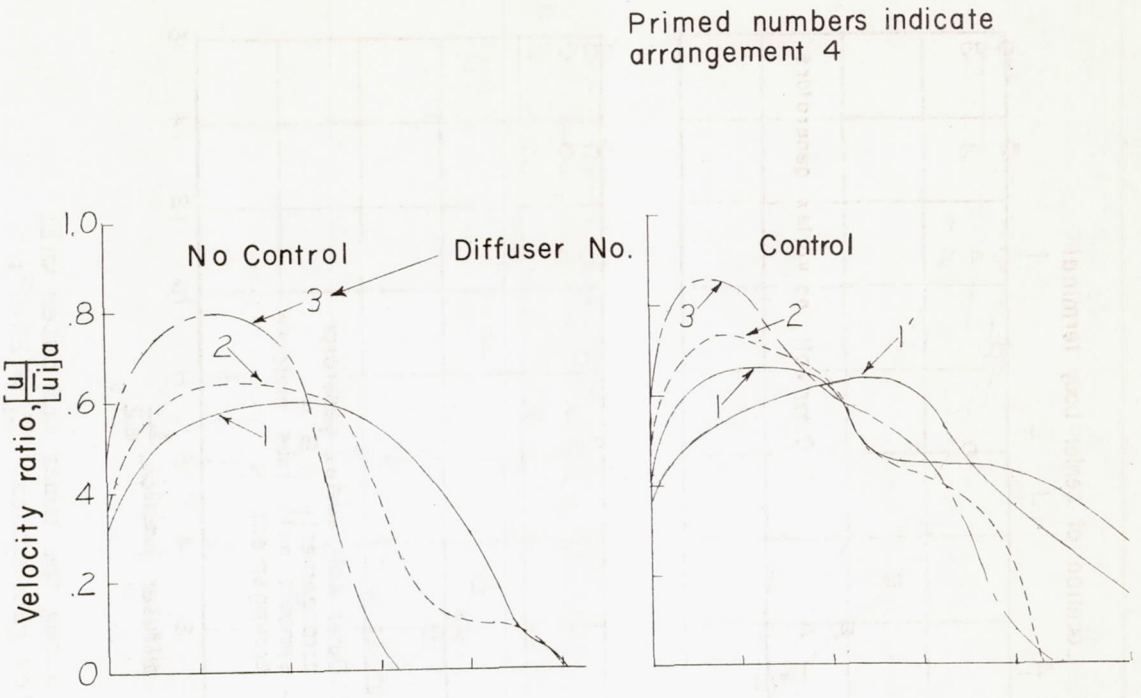

(a) Diffuser-exit station.

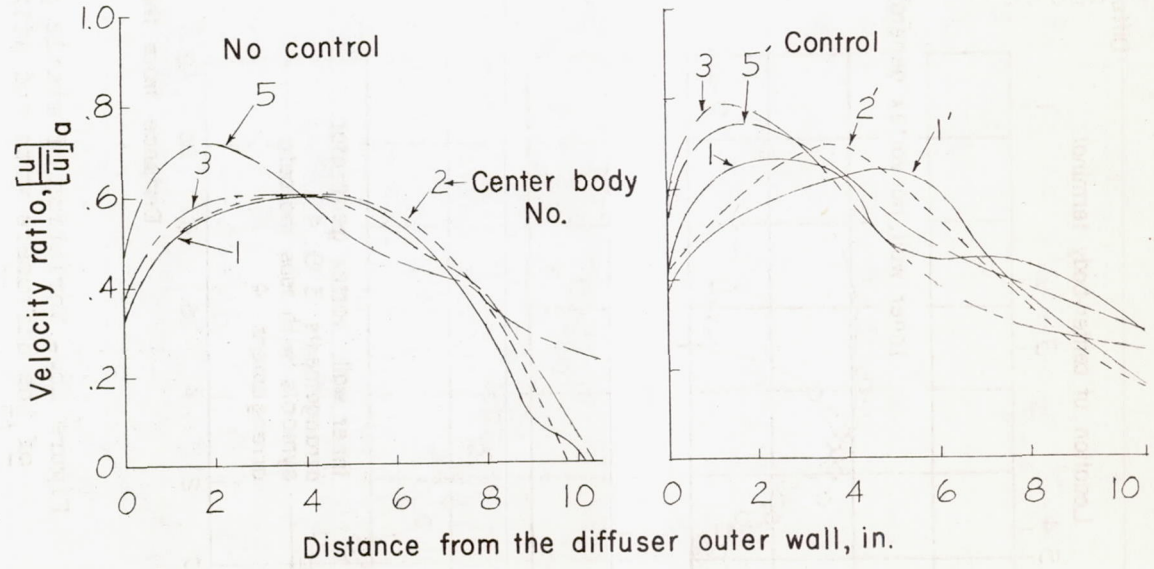

(b) Tailpipe station.

Figure 17.- Radial variation of velocity ratio at the diffuser exit and tailpipe stations for the diffusers with arrangements 3 and 4 and without control. $\bar{X}_i = 20.6^\circ$; $\bar{p}_i / \bar{H}_{ia} = 0.95$.

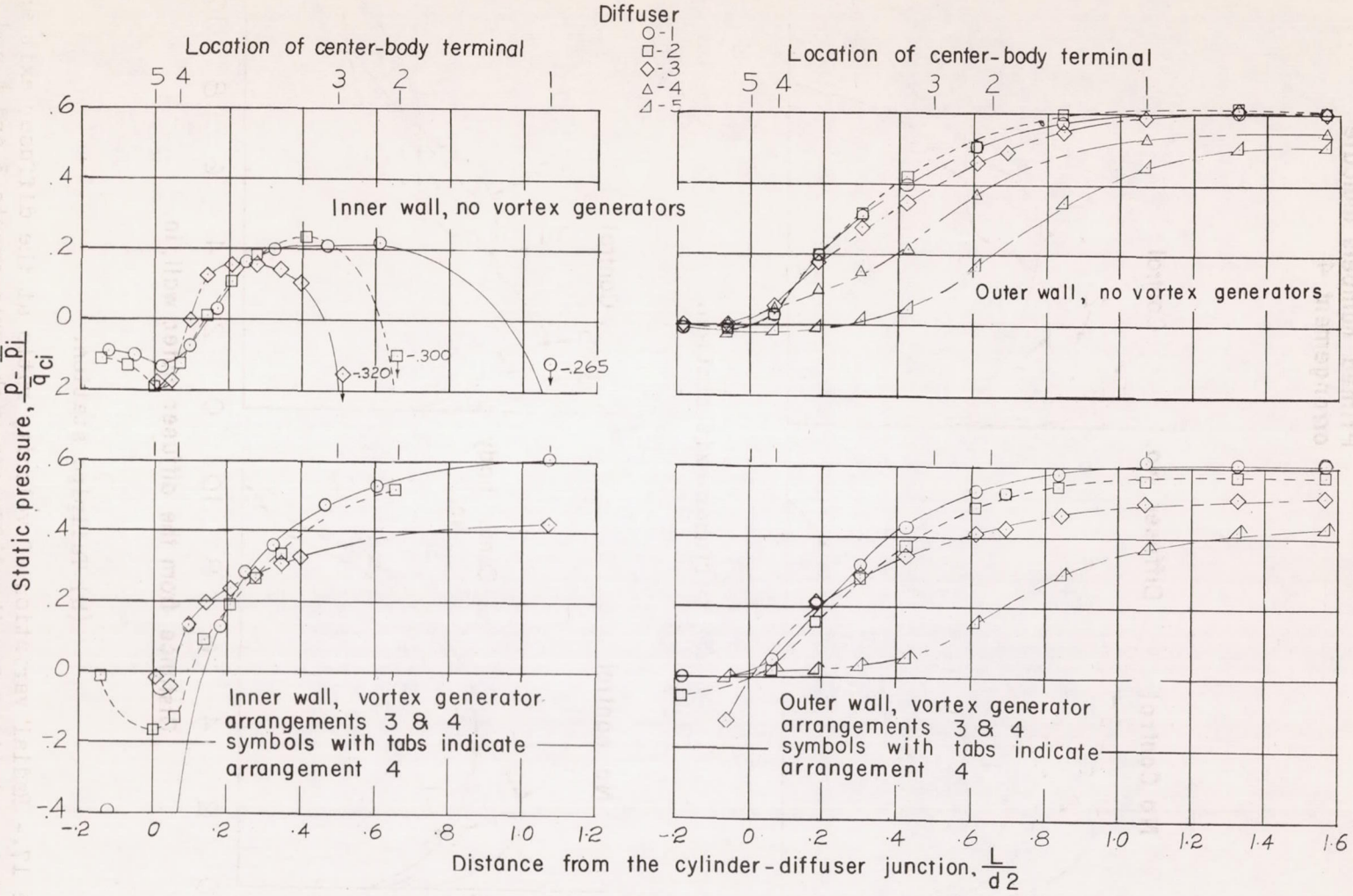

Figure 18.- Variation of static pressure along the inner and outer wall of the diffusers with and without vortex generators. $\bar{X}_i = 20.6^\circ$; $\bar{p}_i/\bar{H}_{ia} = 0.96$.